AMAS WORKSHOP ON ORTHOPAEDIC BIOMECHANICS
OBM'02 – (PP.383–453) – WROCŁAW, SEPTEMBER 1-4, 2002.

Streaming potentials in biological tissues

J.J. TELEGA and R. WOJNAR

Institute of Fundamental Technological Research
Świętokrzyska 21, 00-049 Warszawa, Poland

Streaming potentials and other electrokinetic phenomena based on existence of electrical double layer play an important role in biological processes, especially those occurring in animal tissues. The aim of this paper is to synthesize various contributions and discuss different points of view pertaining to those phenomena.

Key words: *electrical double layer, streaming potentials, biological tissues, bone, cartilage*

1. Introduction

Streaming potentials (SP) arise from a coupling between ion flux and flow of fluid owing to existence of electrical double layer (EDL) and its electric zeta potential (ZP). The role of those potentials in different biological, mechanical, chemical, physical and technological processes is enormous. Particularly, this role is pronounced often in flows through porous media, in sedimentation effects, in particle transport, deposition and aggregation (flocculation), and in colloidal stability of dispersed particles, cf. Hunter [79] and Elimelech *et al.* [38]. Natural streaming potentials arise in soils as the so-called self potentials; electrical streaming potentials are precursors to catastrophic earthquakes. Streaming potential responses caused by oil well pumping are also registered. They are exploited in technology, as in papermaking wet-end chemistry. The SP are essential for life processes. ZP is the basic factor controlling the great majority of aqueous systems, which include blood. It is believed that the stability of blood (its dispersion and gelation) should follow all the precepts which govern the colloids, cf. Riddick [156].

The electrokinetic phenomena are due to the existence of free charges at an interface, *i.e.* the surface of separation of two phases: solid and liquid. The electrical charges, most frequently ions are distributed in a form of two layers of different charges being in contact with the interface. These two layers generate the so-called electrical double layer (EDL).

TABLE 1. Four electrokinetic phenomena

applied electric field causes motion	
ELECTROPHORESIS disperse phase moves liquid phase steady	ELECTROOSMOSIS disperse phase steady liquid phase moves
applied force results in potential	
STREAMING POTENTIAL disperse phase steady liquid phase moves	SEDIMENTATION POTENTIAL disperse phase moves liquid phase steady

An exterior field directed along the interface displaces one ionic layer with respect to the second, thus generating the relative movement of phases. *Vice versa*, the relative movement of phases leads to appearence of a difference of electrical potentials in the direction of relative motion, it is the sedimentation potential or streaming potential.

We distinguish the following electrokinetic phenomena, cf. Table 1:

- Electrophoresis or motion in a liquid of suspension of solid state particles, gas bubbles, drops of another liquid, colloidal particles under influence of exterior electrical field. One may distinguish kata- and anophoresis (towards katode and anode, respectively).
- Electro-osmosis or motion of liquid through capillaries or diaphragms made from solid state material under influence of exterior electric field.
- Sedimentation potential or the potential difference which arises in sedimentation direction as a result of progressive sedimentation of suspended solid state particles.
- Streaming potential or the potential difference which arises between ends of capillary or between surfaces of diaphragm through which a liquid flows.

Electrophoresis and electroosmosis were discovered by Reuss [155] in 1807. The streaming and sedimentation potentials were discovered by Quincke in 1859 and Dorn in 1880, respectively. The streaming potential phenomenon was reported already by Napier in 1846.

The mechanism of SPs depends on the absorption of one type of ions on the surface of the particle (or molecule), with an associate diffuse layer of ions of opposite type extending out from the particle surface. When the liquid stream flows there is a net transport of one type of ion with a resulting potential gradient, which may be measured by means of electrodes placed in

the stream. The magnitude of the SP depends on the type of particles and the pH of solution.

The occurence of an electrical potential difference between the ends of a capillary tube when a fluid flows through was further studied in the nineteenth century, among others, by Wiedemann [202] and Helmholtz [71]. Especially, Wiedemann derived in 1852 the law for flow output, similar to other nonequilibrium phenomenological laws such as the Fourier, Ohm and Darcy laws. Extension of the Helmholtz model to derive electrokinetical velocity was given by Smoluchowski in 1903, cf. [171], [172]. The theory was further developed in by Ghosh [54], Debye and Hückel [30], [31] and Onsager [138]. For the relevant literature the reader is referred to Güzelsu and Demiray [68], Lifshits and Pitayevskiy [103], and Hunter [79].

What concerns biomechanics, after piezoelectric effect was discovered in dry bones in 1953 by Fukada and Yasuda [51], speculation arised that bone remodelling is drived by this effect, cf. also [190]. However, Anderson and Eriksson [3] suggested in 1968 that both bone and tendon have to be bathed *in vivo* in an ionic fluid and the electrical behaviour of wet collagen should be examined. It is not widely known that Iwao Yasuda, MD, (1909-1983) received his PhD in 1950, with a thesis just on streaming potentials, cf. Beadling [8].

Becker *et al.* [12] demonstrated in 1964 that collagen fibres are oriented by weak, direct, electric currents (1μA) as they are reconstituted from solution. The pattern of fibres orientation which occurred near the cathode is field-dependent, and their arrangement is perpendicular to the field. Bassett *et al.* [7] at the same time investigated similar low-level effects of electric currents on bone *in vivo*. These authors found a relationship between electric currents and bone cell activity. Since the seminal paper by Anderson and Eriksson [3], the SPs are believed to be the dominant source of stress-generated potentials in live bone.

The molecular structure of collagen has been described by Ramachandran [150] in 1988. The difference between dry and wet states is brought about by the incorporation of bound water in the wet material. In 1961 Harrington and von Hippel [69] claimed that the crystallinity of collagen, as revealed by X-ray studies, is destroyed by dehydration. Earlier, in 1958, Bradbury *et al.* [17] demonstrated that water molecules attached to collagen constitute an important part of of the diffracting structure. Esipova *et al.* [40] found in the same 1958 that the hydration increased the crystallinity of collagen and oxygen ions of water are arranged in semi-regular fashion along the chains.

Weinbaum *et al.* [199] proposed in 1994 a model for the excitation of osteocytes by mechanical loading-induced bone fluid shear stresses, in which only the Darcy law is exploited, without accounting for electrical pheno-

mena. They predicted pore relaxation time corresponding to times measured by Salzstein and Pollack [167], cf. also Tsay and Weinbaum [191]. More precisely, Weinbaum *et al.* [199] showed that the magnitude of the predicted fluid induced shear stresses is similar to the fluid shear stresses measured in osteoblasts and other cells in which an intercellular Ca^{2+} shear stress response had been observed.

Many different physiological events in both animal and plant cells are regulated by changes in cytoplasmic *p*H (pHc). In animal cells, pHc is well characterized as a regulator of a number of processes, such as modulation of Ca^{2+} signaling (Malayev and Nelson [106]), cytoskeletal polymerisation (Yonezawa *et al.*[207], Suprenant [183], Edmonds *et al.* [37]), longevity of cardiac action potentials (Steidl and Yool [180]). The changes in pHc may include changes in cytoskeletal tension (Grabski *et al.* [57]) and the activity of enzymes involved in signalling. There is an evidence suggesting that changes in pHc can act as a second messenger in plants as well (for a review, see Felle [41], Guern *et al.* [65], Zimmermann *et al.* [213]). Ratiometric wide-field fluorescence microscopy demonstrated that gravistimulation leads to rapid changes in pHc in columella cells of Arabidopsis roots, cf. Scott and Strömgren Allen [168]. There exists also an experimental evidence that the remodelling and regeneration of bone are due to the interaction of both mechanical and electrical forces.

We are going to analyse basic aspects pertaining to the SPs in biological tissues. To be consistent with the topics of this volume we are dealing mainly with processes in animal tissues. In Sect. 2 the most important idea on electroendosmose is given. Double layer properties are discussed in Sect. 3. Theory of ZP is given in Sect. 4 and of SP, including the time-dependent flows and the Levitt theory of flow in narrow channels, is investigated in Sect. 5. Section 6 examines the principles of electrophoresis. The role of SP in development of plant cells is considered in Sect. 7. Section 8 treats peculiarities of SP in cartilage while the most important experiments on SP in wet collagen are described in Sect. 9. Mechanosensory system of bone is sketched in Sect. 10.

2. Heuristic approach to electrical endosmose

Consider a liquid in a container which can be a tube, capillary or pore. On the interface liquid-wall of the container the electrical double layer (EDL) of thickness δ arises. When the liquid is in a state of rest, the electrical potential Ψ produced by the EDL has a constant value Ψ_L in bulk of the liquid and a value Ψ_S in bulk of the solid wall, and changes rapidly in the same layer in the normal direction $\mathbf{n}$ to the wall while remaining constant in the tangent

direction **t**. According to the Gauss theorem the electric charge density ρ^e in the liquid is given by

$$\rho^e = -\varepsilon\varepsilon_0 \frac{\partial^2 \Psi}{\partial n^2}. \tag{2.1}$$

Here ε and ε_0 are electrical permittivities of the liquid and vacuum, respectively.

When the external potential Φ appears, the total electrical potential U is given by $U = \Psi + \Phi$ as we are going to limit ourselves to such slow motions that do not modify the EDL. The force field **F** inducing the motion of liquid is given by

$$\mathbf{F} = \rho^e \mathbf{E} = -\rho^e \nabla \Phi. \tag{2.2}$$

For slow motions we can further neglect the inertial forces and consider the following set of the hydrodynamical equations

$$\nabla p = \eta \Delta \mathbf{v} - \rho^e \nabla \Phi \tag{2.3}$$

where p is the pression in liquid and **v** is the liquid velocity. The analysis of order of magnitude of terms in this equation by Smoluchowski [171] who used the fact that the thickness of EDL being of atomic order is very small in comparison with the dimensions of container, lead him to general result

$$\mathbf{v} = -\varepsilon\varepsilon_0 \frac{\Phi_L - \Phi_S}{\eta} \nabla \Phi \tag{2.4}$$

Introducing the zeta-potential (ZP)

$$\zeta = \Phi_S - \Phi_L \tag{2.5}$$

we get

$$\mathbf{v} = -\frac{1}{\eta} \varepsilon\varepsilon_0 \zeta \mathbf{E}, \tag{2.6}$$

which is known as the Smoluchowski relation. A more detailed analysis is given in Sect.4. Theoretical and experimental investigations of the problem are conducted on possibly simple systems: on metal-liquid systems in which electrical potentials are well defined. In other systems, it arrives that ZP changes from point to point, cf. Fig. 11.

3. Electrical double layer (EDL)

The separation of charge at the interface between two phases is called an electric double layer because it consists of two layers of opposite charge. The concept of EDL is due to Quincke [149], although that term was not used

by him. The simplest model of such system in which both layers of charge are fixed in parallel planes to form a molecular condenser is attributed to Helmholtz [71]. It permits to derive important elektrokinetic relationships, being however oversimplified. Whilst the charges on metal surface may be assumed to be located in a plane (fixed charges), it is not so in a liquid phase where the electrical forces on ions compete with the thermal diffusive forces. The theory of the diffuse double layer was developed independently by Gouy [56] in 1909 and by Chapman [20] in 1913, and subsequently by Stern [181], Debye and Hückel [32], Smoluchowski [173] and Grahame [58]. Recent works on energy of EDL and the Tafel paradox [186], belong to Gokhstein [55].

3.1. Charge distribution in EDL according to Gouy and Chapman

EDL consists of excess ions (or electrons) on the solid phase surface and an equivalent ionic charge of opposite sign in the solution phase near the interface. According to Gouy [56] and Chapman [20] the space charge $\rho^e = \rho^e(\mathbf{x})$ in the solution is given by distribution of point-like ions of valency z_i

$$\rho^e = \sum_i z_i e n_i \tag{3.1}$$

where the sum is taken over all ion kinds i. Moreover, e denotes the elementary electrical charge and n_i is the concentration of ions of kind i.

The Coulomb potential Ψ is given by the Gauss-Poisson equation

$$\Delta\Psi = -\frac{\rho^e}{\varepsilon\varepsilon_0}. \tag{3.2}$$

The solvent is treated as a continuous medium, influencing the double layer only through its dielectric constant ε.

On the other hand, the distribution of ions of kind i and valency z_i is given by the Boltzmann law relating density of ions with the potential Ψ

$$n_i = n_{i0} \exp\left(-\frac{z_i e \Psi}{k_B T}\right). \tag{3.3}$$

Here $n_i = n_i(\mathbf{x})$ is taken at a point $\mathbf{x}$ where the potential $\Psi(\mathbf{x})$ governs, n_{i0} is the concentration in the bulk of solution (where Ψ vanishes), k_B is the Boltzmann constant, and T is the absolute temperature. By combining Eqs. (3.1), (3.2) and (3.3) we get

$$\Delta\Psi = -\frac{1}{\varepsilon\varepsilon_0} \sum_i z_i e n_{i0} \exp\left(-\frac{z_i e \Psi}{k_B T}\right). \tag{3.4}$$

A general solution of this nonlinear equation is not available. If only small values of the potential are accounted for

$$\frac{z_i \mathrm{e}\Psi}{\mathrm{k_B}T} < 1, \tag{3.5}$$

what means that $z_i\Psi < 25\mathrm{mV}$ at the room temperature, then the exponentials may be expanded and only the first two terms retained

$$\exp\left(-\frac{z_i \mathrm{e}\Psi}{\mathrm{k_B}T}\right) = 1 - \frac{z_i e\Psi}{\mathrm{k_B}T}.$$

Then Eq.(3.4) is linear

$$\Delta\Psi = \kappa^2\Psi, \tag{3.6}$$

where

$$\kappa^2 = \frac{\mathrm{e}^2}{\varepsilon\varepsilon_0 \mathrm{k_B}T}\sum_i n_{i0} z_i^2, \tag{3.7}$$

and the electroneutrality of the solution was taken into account

$$\sum_i z_i e n_{i0} = 0.$$

Applicability of Eq. (3.6) was discussed by several authors such as Onsager [138] in 1927, Kirkwood in 1934, Casimir in 1944, Fowler and Guggenheim in 1949, Overbeek in 1952, cf. [139].

3.2. One-dimensional case

Consider now an infinite interface, so that the Laplace operator Δ simplifies to d^2/dx^2 and Eq.(3.4) takes the form

$$\frac{d^2\Psi}{dx^2} = -\frac{1}{\varepsilon\varepsilon_0}\sum_i z_i e n_{i0} \exp\left(-\frac{z_i \mathrm{e}\Psi}{\mathrm{k_B}T}\right). \tag{3.8}$$

In this 1D case the nonlinear equation (3.8) can be solved analytically. After multiplying both sides of the last equation by $d\Psi/dx$ we have

$$\frac{d\Psi}{dx}\frac{d^2\Psi}{dx^2} = -\frac{1}{\varepsilon\varepsilon_0}\sum_i z_i e n_{i0} \exp\left(-\frac{z_i \mathrm{e}\Psi}{\mathrm{k_B}T}\right)\frac{d\Psi}{dx}. \tag{3.9}$$

Integration gives

$$\frac{1}{2}\left(\frac{d\Psi}{dx}\right)^2 = \frac{\mathrm{k_B}T}{\varepsilon\varepsilon_0}\sum_i n_{i0} \exp\left(-\frac{z_i \mathrm{e}\Psi}{\mathrm{k_B}T}\right)\frac{d\Psi}{dx} \tag{3.10}$$

where the conditions

$$\Psi \to 0, \quad \frac{d\Psi}{dx} \to 0 \quad \text{for} \quad x \to \infty$$

have been imposed.

A simple specific case is a single binary electrolyte of valency z in the solution where

$$n_{i0} \equiv n \quad \text{and} \quad z_i = \pm z$$

and, cf. Eq.(3.7),

$$\kappa^2 = \frac{2nz^2\mathrm{e}^2}{\varepsilon\varepsilon_0 \mathrm{k_B} T}. \tag{3.11}$$

From Eq.(3.10) we then get

$$\frac{d\Psi}{dx} = -\sqrt{2n\frac{\mathrm{k_B}T}{\varepsilon\varepsilon_0}}\left[\exp\left(\frac{ze\Psi}{2\mathrm{k_B}T}\right) - \exp\left(-\frac{ze\Psi}{2\mathrm{k_B}T}\right)\right]. \tag{3.12}$$

Integration of the last equation yields

$$\int_{\Psi_0}^{\Psi} \frac{\frac{ze}{2\mathrm{k_B}T}d\Psi}{\exp\left(\frac{ze\Psi}{2\mathrm{k_B}T}\right) - \exp\left(-\frac{ze\Psi}{2\mathrm{k_B}T}\right)} = -ze\sqrt{\frac{n}{2\varepsilon\varepsilon_0\,\mathrm{k_B}T}}\int_0^x dx$$

or, after (3.11),

$$\int_{\Psi_0}^{\Psi} \frac{\frac{ze}{\mathrm{k_B}T}d\Psi}{\exp\left(\frac{ze\Psi}{2\mathrm{k_B}T}\right) - \exp\left(-\frac{ze\Psi}{2\mathrm{k_B}T}\right)} = -\kappa x. \tag{3.13}$$

Finally we arrive at

$$\kappa x = \ln\frac{[\exp\left(\frac{ze\Psi}{2\mathrm{k_B}T}\right)+1][\exp\left(\frac{ze\Psi_0}{2\mathrm{k_B}T}\right)-1]}{[\exp\left(\frac{ze\Psi}{2\mathrm{k_B}T}\right)-1][\exp\left(\frac{ze\Psi_0}{2\mathrm{k_B}T}\right)+1]}. \tag{3.14}$$

Thus an explicit relation between the potential and the coordinate in the double layer has been found. In the case of *small* potentials this relation simplifies to

$$\Psi = \Psi_0 e^{-\kappa x}. \tag{3.15}$$

We conclude that the potential drops exponentially with the decay length $1/\kappa$, known also as the Debye-Hückel or simply - the Debye length.

3.3. Surface charge density η_0^e and surface potential Ψ_0 in 1D

The condition of electroneutrality of the double layer requires that the surface charge be equal but opposite to the total space charge in the solution

$$\eta_0^e = -\int_0^\infty \rho^e dx. \tag{3.16}$$

According to Eq.(3.2) $\rho^e = -\varepsilon\,\varepsilon_0 \Delta\Psi$ and in the 1D case we get

$$\rho^e = -\varepsilon\,\varepsilon_0 \frac{d^2\Psi}{dx^2}. \tag{3.17}$$

Equations (3.12), (3.16) and (3.17) result in

$$\eta_0^e = \sqrt{2\varepsilon\,\varepsilon_0 n\,\mathrm{k_B}T}\left(e^{\frac{ze\Psi_0}{2\mathrm{k_B}T}} - e^{-\frac{ze\Psi_0}{2\mathrm{k_B}T}}\right). \tag{3.18}$$

For *small* values of the potential we get

$$\eta_0^e = \sqrt{2\varepsilon\,\varepsilon_0 n\,\mathrm{k_B}T}\cdot\frac{ze\Psi}{\mathrm{k_B}T} = \varepsilon\,\varepsilon_0\kappa\,\Psi_0. \tag{3.19}$$

In this case the charge and potential are proportional and the double layer behaves as a flat condenser with a distance $1/\kappa$ between two plates (as in the Wiedemann theory). This primal fact justifies treating the thickness of EDL to be equal to the Debye length $1/\kappa$.

3.4. EDL in capillaries

The interfacial tension of a solid (metal) in contact with aqueous solution of electrolyte in a capillary varies with the potential difference Φ imposed across the interface. This dependence is known as the electrocapillary curve and may be studied with help of a device known as the capillary electrometer, cf. Feoktistov [43].

Schematic representation of electrometer is shown in Fig. 1. Denote after Grahame [58] by $\Psi^I, \Psi^{II}, \Psi^\alpha$ and Ψ^β the potentials of the several elements. It is evident that

$$\Phi + (\Psi^\alpha - \Psi^I) + (\Psi^\beta - \Psi^\alpha) + (\Psi^{II} - \Psi^\beta) = 0. \tag{3.20}$$

Metallic phase α does not alter in the process, so that $(\Psi^\alpha - \Psi^I)$ is a constant and we may write

$$d(\Psi^\beta - \Psi^\alpha) = -d\Phi - d(\Psi^{II} - \Psi^\beta). \tag{3.21}$$

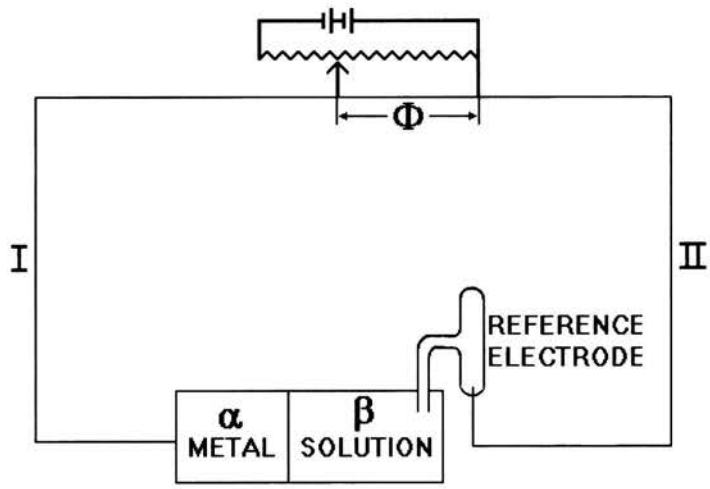

FIGURE 1. Schematic representation of electrometer: I and II are wires of the same metallic substance, α is the metallic phase in contact with the electrolytic solution β; after Grahame [58]

The basic equation derived from the Gibbs adsorption equation is

$$d\sigma = \eta^e d(\Psi^\beta - \Psi^\alpha) - \sum_i \Gamma_i d\mu_i, \tag{3.22}$$

where σ is the interfacial tension of two immiscible phases, μ_i is the chemical potential (partial molal free energy at constant temperature T and pressure p) of a component no i, Γ_i is the excess of the component (in moles per unit area of interface) over that which would be present in the system if each phase were of uniform composition with the composition of the interior of the phase, and η^e is the surface charge density of electricity on the metallic phase. The definition of η^e used in the derivation of (3.22) is

$$\eta^e = -\mathrm{F} \sum_i^\beta \Gamma_i z_i \tag{3.23}$$

where the summation is limited to the ions of the non-metallic phase, F is the Faraday constant, z_i is the valence of component i. Therefore η^e is equal to the total charge of the ions of the double layer. By Eq.(3.21) we have

$$d\sigma = -\eta^e d\Phi - \eta^e d(\Psi^{II} - \Psi^\beta) - \sum_i \Gamma_i d\mu_i. \tag{3.24}$$

At constant composition, $d\mu_i = 0$ for each component and $d(\Psi^{II} - \Psi^\beta) = 0$.

Hence we get the Lippmann equation from 1875, cf. [104],

$$\eta^e = -\left.\frac{d\sigma}{d\Phi}\right|_{p,T,\mu} \tag{3.25}$$

It states that the slope of the electrocapillary curve is equal to the electric charge density of the metallic surface, cf. Fig. 2. From (3.25) it follows that at the potential of the electrocapillary maximum $\eta^e = 0$. The rate of change

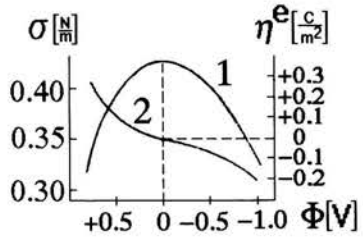

FIGURE 2. Electrocapillary curve $\sigma = \sigma(\Phi)$ (1) and the dependence of surface charge density η^e on the potential Φ (2). The potential difference between mercury and electrolyte is arbitrarily set equal zero at the electrocapillary maximum; after [58] and [44].

of the slope of the electrocapillary curve is

$$\left.\frac{d^2\sigma}{d\Phi^2}\right|_{p,T,\mu} = -\left.\frac{d\eta^e}{d\Phi}\right|_{p,T,\mu} = C \tag{3.26}$$

where C is the differential capacity of the double layer.

3.5. Stern-Grahame approach

The characteristic length $1/\kappa$ is of the order of molecular dimensions (several angstroms). Ions in solutions are not point charges, but have a finite size. Hydrated ions have the diameters of order of 5Å=0.5nm. Therefore the Gouy and Chapman assumption that the electrolyte ions can be treated as point charges is unsatisfactory. The finite size of ions limits their maximum concentration at the wall, and their distance of closest approach to it.

The current theories of EDL based on Stern [181] concepts from 1924 divide the space charge in the electrolyte into two regions: the inner region very near to wall in which the charge distribution is determined chiefly by the geometrical restrictions of ion size, and the outer region where the Poisson-Boltzmann equation gives reasonable solution of the problem, cf. [181].

If ion charge is located at the center of a sphere of finite size, the charge cannot touch the interface, and must be limited to a distance δ of approach of

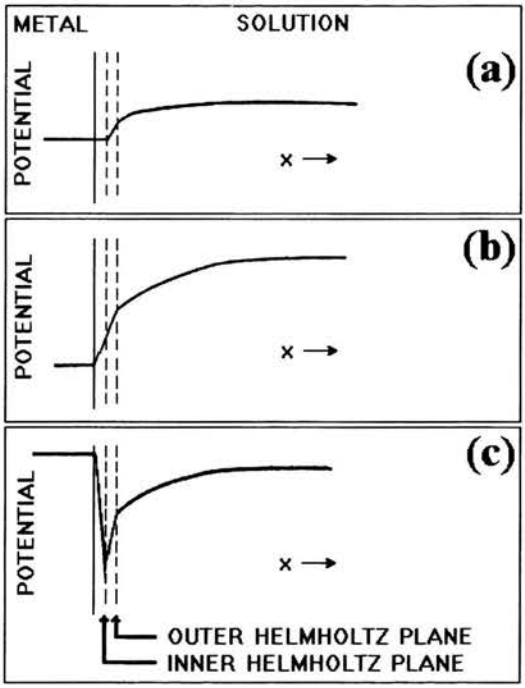

FIGURE 3. (a) Schematic representation of the EDL at the potential of the electrocapillary maximum (cf. Fig. 2); (b) Schematic representation of the EDL with negative polarization; (c) Schematic representation of the EDL with positive polarization; diffuse double layer is identical with that depicted in Fig. (b); after [58].

the order of the sphere radius. The plane at distance δ is known as the Stern plane. The Stern plane may be regarded as one of the planes of a capacitor, the capacitance of which depends on its thickness δ and permittivity of the medium close to the surface.

Further refinement of the theory (1947), due to Grahame [58], subdivides the Stern layer into two regions: an inner layer occupied by unhydrated ions (inner sphere complexes) and a second layer where hydrated counterions (outer sphere complexes) are located. The boundaries of these regions are known as the inner Helmholtz plane (IHP) and outer Helmholtz plane (OHP). The OHP is equivalent to the Stern plane, see Figs. 3 and 4. In aqueous systems the permittivity of water close to a charged interface is significantly lower than the bulk value. The relative permittivity ε (the dielectric constant) of bulk water is about 78 whilst at the surface (for $\delta = 0.3$nm) it is reduced to $\varepsilon \approx 10$, see Fig. 4.

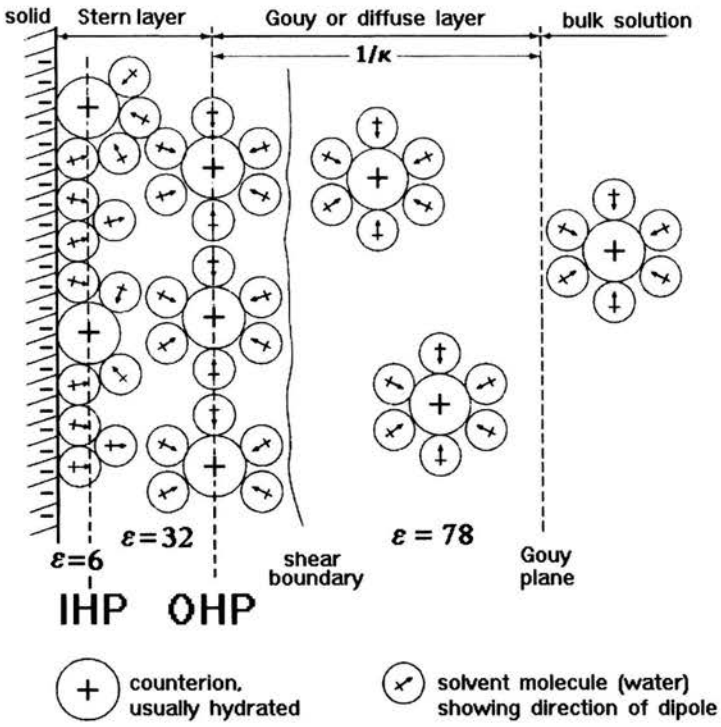

FIGURE 4. The potential distribution at an interface (near a metal electrode). The plane of centres of anions is called the inner Helmholtz plane (IHP) and that of cations is called outer Helmholtz plane (OHP). The shear plane lies very close to OHP. In some non-metalic system the majority of countercharge (up to 90%) appears to lie between the solid surface and the OHP; after Elimelech *et al.* [38].

4. Zeta potential

4.1. Zeta potential at flat wall

We consider the movement of liquid adjacent to a flat, charged surface under the influence of an electric field $\mathbf{E} = (0, 0, E_z)$ applied parallel to the interface.

If the charge on the surface is negative, there will be a net excess of positive ions in the adjacent liquid. These ions, as they move under the influence of the applied field $\mathbf{E}$, will draw the liquid along with them. The direction of flow is the z-axis, parallel to the wall; x-axis is perpendicular to the wall. Stationary state is reached after a short starting period and each layer, dx, of the liquid moves with a uniform velocity parallel to the wall, because the total force on such a layer is zero. The slipping plane or the

surface of shear is in this case taken as a plane parallel to the surface at the distance δ, see Fig. 5.

The shear surface is an imaginary surface which is considered to lie close to the solid surface and within which the fluid is stationary. In the case of particle undergoing electrophoresis the shear surface forms a sheath which envelopes the particle. The average potential on the surface of shear is called the electrokinetic or ζ potential, ZP for short.

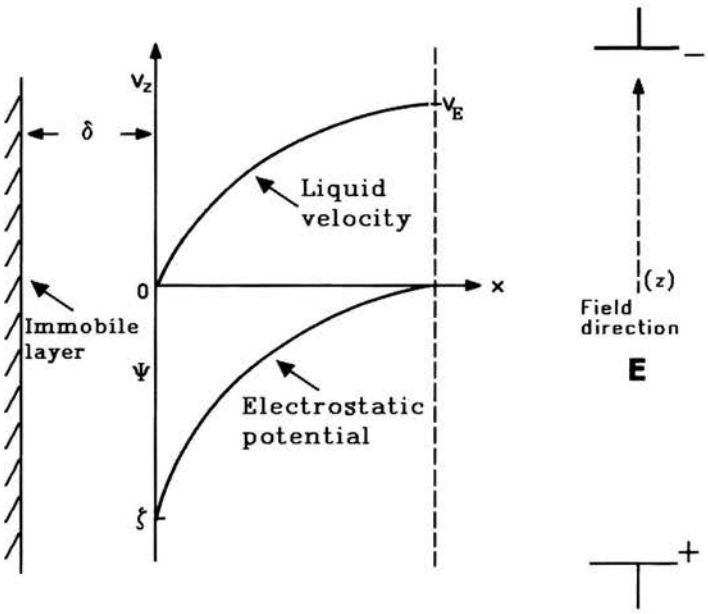

FIGURE 5. Electrostatic potential Ψ near a charged surface and the resulting electro-osmotic velocity v_E under an applied field $\mathbf{E} = (0, 0, E_z)$. The velocity of liquid v_z rises from a value of zero in the plane of shear to a maximum value v_E at some distance from the wall, after Hunter [79].

Let the velocity of the liquid be $\mathbf{v} = (0, 0, v_z)$ and the viscosity be denoted by η. The velocity gradient in the x-direction generates the shear stress $\sigma_{xz} = \eta\, dv_z/dx$. Under shear each element of the liquid has neighbouring elements moving with different velocities - on one side more slowly than on the other. The net force applied per unit area is

$$\eta \left(\frac{dv_z}{dx}\right)_{x+dx} - \eta \left(\frac{dv_z}{dx}\right)_x = \eta \frac{d^2 v_z}{dx^2} dx.$$

The electric charge per unit area is $\rho^e dx$ and the electric force acting on this area in the field $\mathbf{E} = (0, 0, E_z)$ is $E_z \rho^e dx$. In the stationary state the forces

acting on the given element of the liquid are equilibrated

$$\rho^e E_z = \eta \frac{d^2 v_z}{dx^2}. \tag{4.1}$$

By using the Gauss-Poisson equation (3.17) we find

$$-E_z \varepsilon\varepsilon_0 \frac{d^2\Psi}{dx^2} = \eta \frac{d^2 v_z}{dx^2}. \tag{4.2}$$

This equation has to be integrated over the whole liquid, that is between $x = \infty$ and the slipping plane. The following boundary conditions are imposed

$$\Psi_\infty = 0, \qquad \left(\frac{d\Psi}{dx}\right)_\infty = 0, \qquad \left(\frac{dv_z}{dx}\right)_\infty = 0 \quad \text{for } x = \infty,$$

$$\Psi = \zeta, \qquad v_z = 0 \qquad \text{for the slipping plane.} \tag{4.3}$$

The first integration shows that the velocity gradient and the potential gradient are always proportional, cf. Fig. 5. Denoting by v_E the velocity of the liquid at a large distance from the wall, we find

$$v_E = -\varepsilon\varepsilon_0 \frac{\zeta}{\eta} E_z. \tag{4.4}$$

This velocity is called *the electroosmotic* or *Smoluchowski velocity.* The electroosmotic mobility is defined by

$$u_E \equiv \frac{v_E}{E_z}. \tag{4.5}$$

Hence, from Eq.(4.4) we get

$$u_E = -\varepsilon\varepsilon_0 \frac{\zeta}{\eta}. \tag{4.6}$$

The negative sign indicates that when ζ is negative the space charge is positive and the liquid flow is directed towards the negative electrode.

4.2. Meaning of zeta potential in 2D flow

Recently Dutta and Beskok [34] treated the problem of the mixed electroosmotic and pressure driven flow in 2D flat channel at presence of ZP. Figure 6 depicts the velocity profile in this channel described by the equation

$$v(\xi) = -\frac{1}{2}\frac{\Pi}{\lambda}(1 - \xi^2) + 1 - \psi^*(\xi), \tag{4.7}$$

in which rescaled variables are used

$$\xi = \frac{x}{h}, \quad \lambda = \frac{\ell}{h}, \quad \upsilon = \frac{v_z}{v_E}, \quad \Pi = \frac{p}{\eta v_E/h} \quad \text{and} \quad \psi^* = \frac{\Psi}{\zeta},$$

where h is the half channel width and ζ is ZP.

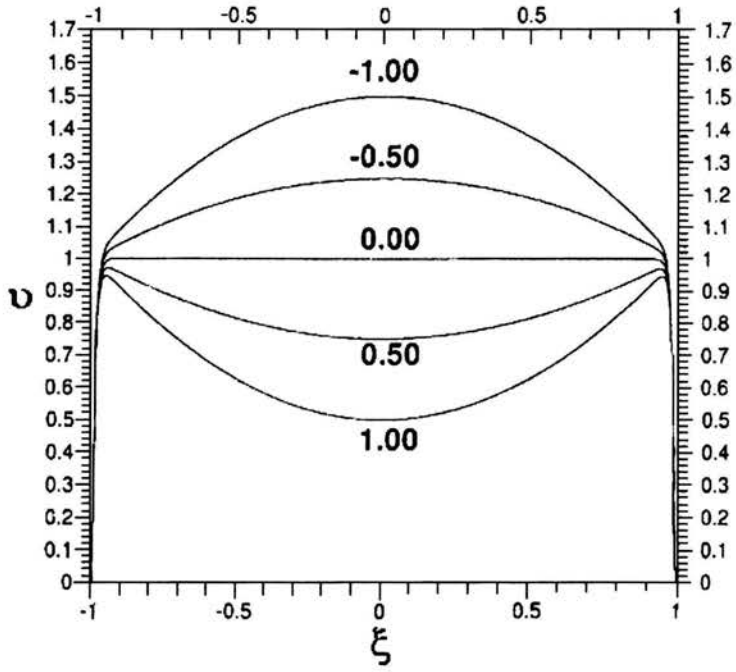

FIGURE 6. Velocity distribution across the channel in mixed electroosmotic/pressure driven flow under various values of the streamwise pressure gradient $\Pi\lambda$, cf. Eq. (4.7) and Fig. 8; after Dutta and Beskok [34].

In the analysis of EDL region near the walls Dutta and Beskok [34] have shown that electroosmotic velocity (4.4) can be used as an approximate slip velocity on the wall (if one neglects the velocity distribution within the EDL).

Dutta *et al.* [35] performed numerical simulation of electroosmotically driven flows in grooved micro-channels and compared numerical results with experimental measurements. The model of EDL used by those authors was simplified. Comparison shows good agreement validating both numerical and experimental methods. The Brownian motion error was estimated to be as small as 0.6%. Similarities between the electric field lines and streamlines were observed. The last are shown in Fig. 7.

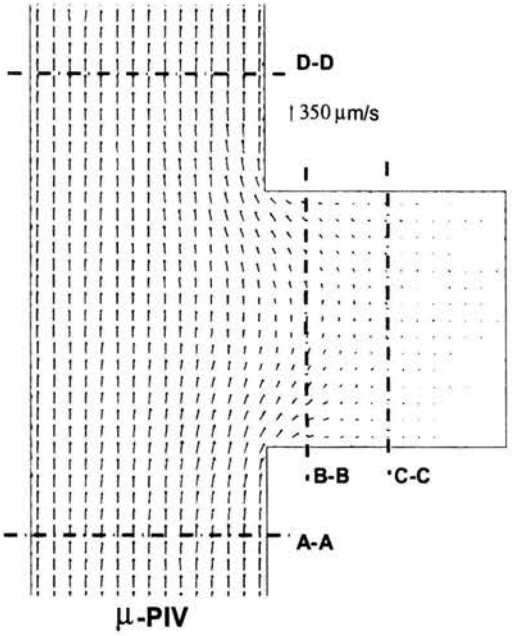

FIGURE 7. Streamlines and velocity vectors for the grooved micro-channel obtained with help of microscopic particle image velocimetry (μ-PIV). We observe a uniform plug-like flow in the upstream (A-A section) and downstream (D-D section) of the grove. In these regions the flow is unidirectional, while the flows near the groove corners show two-dimensional flow (B-B and C-C sections), after Dutta *et al.* [35].

4.3. Zeta potential in capillaries

In a capillary with cylindrical symmetry the Laplace operator acting on a function $f = f(r)$ has the form $\Delta f = \frac{1}{r}\frac{df}{dr} + \frac{d^2f}{dr^2}$. The thickness δ of the EDL is on the order of $1/\kappa$, thus on the order of nanometer, cf. Fig. 8. In capillaries this layer situated in the ring $R - \delta < r < R$ is very thin compared to the capillary radius ($10^{-3}\text{cm} < R < 10^{-1}\text{cm}$). One may assume that $R \to \infty$ and the results obtained for a flat surface are applicable to the capillary wall surface.

The Gauss-Poisson equation (3.2) for the potential Ψ takes the form

$$\rho^e = -\varepsilon\varepsilon_0 \frac{d^2\Psi}{dr^2}. \tag{4.8}$$

For a capillary with constant cross-section according to the definition of elec-

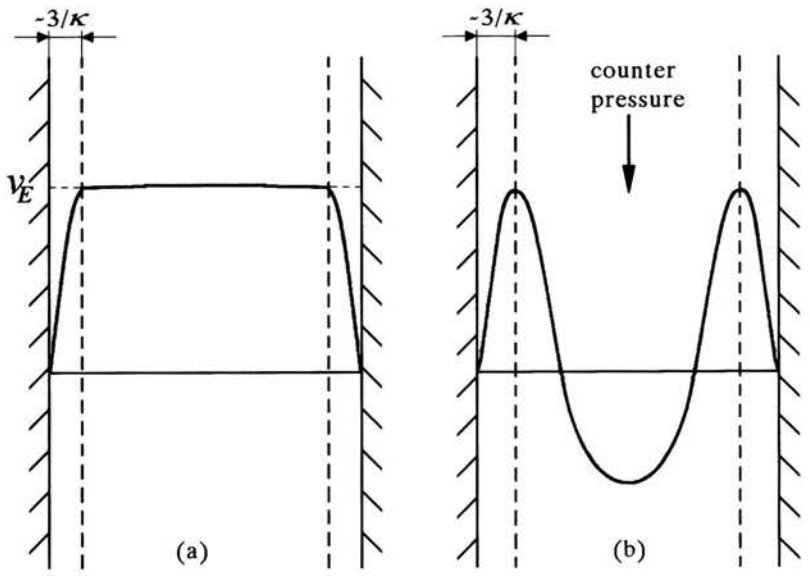

FIGURE 8. Velocity profile in a capillary during: electro-osmosis (a) and electro-osmotic counter pressure measurement (b). The thickness of the layer of varying velocity at the wall has been greatly exaggerated. As its thickness is of order of nanometers, it can not be visible with an ordinary microscope and all of the liquid near wall appears to move with the velocity v_E, after Hunter [79].

troosmotic velocity (4.4), the fluid volume displaced per unit time is

$$J = \pi R^2 v_E = \pi R^2 \varepsilon\varepsilon_0 \frac{\zeta}{\eta} E_z. \tag{4.9}$$

The electric current I transported by the liquid is

$$I = \pi R^2 \lambda_0 E_z \tag{4.10}$$

where λ_0 denotes the electrical conductivity. Hence

$$\frac{J}{I} = \frac{\varepsilon\varepsilon_0}{\lambda_0} \frac{\zeta}{\eta}. \tag{4.11}$$

This equation is valid provided that the flow is laminar. The flow described by Eq. (4.11) is generated by electroosmosis, so it proceeds without pressure difference, *i.e.* $P = 0$.

5. Streaming potentials

If the pressure difference $P = p_1 - p_2$ enforces liquid to flow through a capillary, the charges in the mobile part of the double layer near the wall are

carried with the liquid. Then the streaming current I_s arises and the accumulation of charges sets up an electric field. The field causes the conduction current I_c to flow in the opposite direction through the bulk of the liquid, see Fig. 11. If $I_s + I_c = 0$, a steady state is achieved. The resulting electrostatic potential difference between the ends of the capillary is the streaming potential (SP). The current I_s in a cylindrical tube (capillary) is

$$I_s = \int_0^R v_z(r)\rho^e(r)2\pi r dr. \tag{5.1}$$

The velocity $v_z = v_z(r)$ of the liquid is given by the Hagen-Poiseuille relation which can be approximated as follows

$$v_z = v_z(r) = \frac{1}{4\eta}\frac{P}{\ell}(R-r)(R+r) \approx \frac{1}{2\eta}\frac{P}{\ell}R(R-r), \tag{5.2}$$

because the values of r close to R give only the contribution to the integral (5.1) (the bulk of the moving liquid carries no net charge). Furthermore, if ρ^e is substituted after the Gauss-Poisson equation (4.8) we get

$$I_s = \frac{1}{2\eta}\frac{P}{\ell}R(-1)\varepsilon\varepsilon_0 \int_0^R (R-r)\frac{d^2\Psi}{dr^2}2\pi r dr.$$

Since the double layer is confined to a thin region near the wall of the capillary, only the values of r close to $r = R$ are of importance in the determination of the current. Hence

$$I_s = -\varepsilon\varepsilon_0\frac{\pi R^2}{\eta}\frac{P}{\ell}\int_0^R (R-r)\frac{d^2\Psi}{dr^2}dr = -\varepsilon\varepsilon_0\pi R^2\frac{\zeta}{\eta}\frac{P}{\ell}. \tag{5.3}$$

Here it has been assumed that for $r = 0$, $\Psi = 0$ and $d\Psi/dr = 0$, whilst for $r = R$, $\Psi(R) \approx \Psi(R-a) \equiv \zeta$. The streaming potential Φ_s generated by the current I_s causes a conduction current in the reverse direction

$$I_c = \pi R^2\lambda_0 E_z = \pi R^2\lambda_0\frac{\Phi_s}{\ell}, \tag{5.4}$$

where λ_0 is the electrical conductivity of the liquid. In a steady state $I = I_s + I_c = 0$ or $\varepsilon\varepsilon_0(\zeta/\eta)P = \lambda_0\Phi_s$. Hence we get

$$\frac{\Phi_s}{P} = \varepsilon\varepsilon_0\frac{\zeta}{\eta\lambda_0}. \tag{5.5}$$

Comparing (5.5) with (4.11) we conclude that

$$\left(\frac{\Phi_s}{P}\right)_{I=0} = \left(\frac{J}{I}\right)_{P=0}. \tag{5.6}$$

This relationship, due to Mazur and Overbeek (1951), is an example of the Onsager principle of reciprocity, cf. [116].

From Eq. (5.5) we get that the SP is proportional to the force $\mathcal{F}$ acting on the fluid

$$\Phi_s = \varepsilon\varepsilon_0 \frac{\zeta}{\eta} \frac{1}{\lambda_0 A} \mathcal{F}, \tag{5.7}$$

where $\mathcal{F} = AP$ and A is the area of the sample disc through which the electrolyte flows. According to the Hagen-Poiseuille law, the output volume (volume flux) is given by $J = [\pi/(8\eta)]R^4(P/\ell)$ and the mean value of the liquid velocity is expressed by $\bar{v} = J/(\pi R^2) = R^2/(8\eta\ell)A^{-1}\mathcal{F}$. Hence $\mathcal{F} = R^{(-2)}8\eta\ell A\bar{v}$. Substituting this into (5.7) we get

$$\Phi_s = \varepsilon\varepsilon_0 \frac{\zeta}{\lambda_0} \frac{8}{R^2} \ell\bar{v}. \tag{5.8}$$

Thus the SP is proportional to the mean velocity $\bar{v}$ of the fluid.

5.1. Streaming potentials in capillaries for variable pressure

The simplest case of nonsteady flow of viscous liquid through cylindrical tube was considered already in 1879 by Helmholtz [71], see also Gromeka [59], Szymanski [185] and Loytsianskiy [105]. The extension of the SP theory to the case for sinusoidal flow was given by Packard [141] in 1953.

The Stokes equation for the liquid with the density ρ and viscosity η in axisymmetrical case for the velocity v_z reads

$$\rho\frac{\partial v_z}{\partial t} - \eta\Delta v = -\frac{\partial p}{\partial z}. \tag{5.9}$$

For the displacement w_z in the direction z, for the liquid subjected to a uniform driving force $P\exp(-i\omega t)$ at one end, varying in time t with frequency ω, we get

$$\eta\frac{1}{r}\frac{\partial}{\partial r}\left(r\frac{\partial^2 w_z}{\partial r\partial t}\right) - \rho\frac{\partial^2 w_z}{\partial t^2} = -\frac{P}{\ell}\exp(-i\omega t), \tag{5.10}$$

because $v_z = \partial w_z/\partial t$. Solution of Eq. (5.10) for the boundary condition $v_z = 0$ at $r = R$ is

$$v_z = \frac{i}{\omega}\frac{1}{\rho}\frac{P}{\ell}\left[\frac{J_0(kr)}{J_0(kR)} - 1\right]\exp(-i\omega t), \tag{5.11}$$

where $J_0(kr)$ is the Bessel function of the first kind and $k^2 = i\omega\rho/\eta$.

The Gauss-Poisson Eq. (3.2) for Ψ depending only on r assumes the form

$$\frac{1}{r}\frac{d}{dr}\left(r\frac{d\Psi}{dr}\right) = -\frac{\rho^e}{\varepsilon\varepsilon_0}. \tag{5.12}$$

Combining (5.15) with (5.14) in (5.1) we get

$$I_s = \int_0^R \frac{i}{\omega}\frac{1}{\rho}\frac{P}{\ell}\left[\frac{J_0(kr)}{J_0(kR)} - 1\right] e^{(-i\omega t)} \times \left[-\varepsilon\varepsilon_0\frac{1}{r}\frac{d}{dr}\left(r\frac{d\Psi}{dr}\right)\right] 2\pi r dr. \tag{5.13}$$

Integrating by parts we obtain

$$I_s = -\frac{2\pi i}{\omega}\varepsilon\varepsilon_0\zeta\frac{1}{\rho}\frac{P}{\ell}kR\frac{J_1(kR)}{J_0(kR)}\exp(-i\omega t). \tag{5.14}$$

The agreement between theory and experiment for glass samples tested by Packard was quite satisfactory.

Extension of the description to include the full set of Maxwell equation was done by Pride [145] in 1994 who, starting from the first principles, has derived equations that describe such *electroseismic* phenomena when an electrokinetic coupling mechanism appears. The coupling is due to an excess of electrolyte ions that exist in a fluid layer near the grain surfaces within the material. When a mechanical wave propagates through the medium, a relative fluid-solid motion is induced that transports counterions relative to the fixed charge thus inducing an electrical streaming current which is a source of SP, cf. also Pride and Haartsen [146], Pride and Garambois [147].

Reppert *et al.* [154] constructed in 2001 an experimental device and data acquisition system to measure the streaming potential coupling coefficients as a function of frequency. The purpose of the experiments was to measure, for the first time, the real and imaginary portion of streaming potentials. Frequency-dependent streaming potential experiments were conducted on one glass capillary and two porous glass filters. Two frequency-dependent models (Packard and Pride) were compared to the data. Both Pride's and Packard's models have a good fit to the experimental data in the low- and intermediate-frequency regime. In the high-frequency regime, the data fit the theory after being corrected for capacitance effects of the experimental setup. Pride's generalized model appears to have the ability to more accurately estimate pore sizes in the porous medium samples, Packard's model has one unknown model parameter while Pride's model has four unknown model parameters, two of which can be independently determined experimentally. Pride's additional parameters allow for a determination of permeability.

5.2. Streaming potential in narrow channels

Channels with 3-4Å in diameter found, for instance, in kidney and cartilage are comparable with the diameter of water molecule. It was recognized in 1978 in paper by Levitt *et al.* [98] that for the special case of a channel that was so narrow that the water and ion could not pass each other ("no pass channel") a rigorous relation could be derived that relates the SP to the number of ions in the channel. Probably the most judicious assessment of the present state theory of ion passage through such narrow channel is given recently by Levitt [99]- [101].

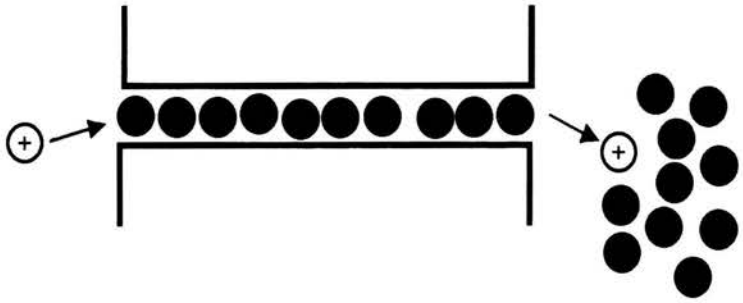

FIGURE 9. A model of no pass channel. The black filled circles represent the water molecules, after Levitt [101].

It is clear from Fig. 9 that in the case when n is a number molecules in the channel per one ion, each ion that crosses the channel must displace n water molecules.

The following general relationship for the streaming potential Φ_s in this case can be derived

$$\left(\frac{\Phi_s}{P}\right)_{I=0} = \left(\frac{J}{I}\right)_{P=0} = \frac{1}{ze}\left(\frac{J}{J_s}\right) = \frac{1}{ze}V_i = \frac{V_w}{zF}n, \tag{5.15}$$

where P is the pressure difference, J_s is ion flux (the number of ions per second), J is the volume flux (ml/second), V_i is the volume per ion which is equal n times the volume of water molecule, V_w is the molar volume of water. The first equality makes use of the Mazur and Overbeek equality (5.6).

It can be shown that for narrow (no pass) channels the Smoluchowski classical SP relation remains valid. Furthermore, the continuum Poiseuille law remains approximately valid in pores with dimensions of a few water molecules. Probably it is correct to within a factor of 2, cf. Levitt [101].

6. Electrophoresis

The analysis of electroosmosis expounded earlier is also applicable to electrophoretic motion of a large particle with a thin double layer. Regarding the liquid as fixed, so that particle moves in the opposite direction, we find the particle mobility, cf. Eq. (4.6),

$$u_E = \varepsilon\varepsilon_0 \frac{\zeta}{\eta}. \tag{6.1}$$

This is the Smoluchowski expression for the electrophoretic mobility. Hückel [75] re-examined in 1924 the problem and found similar relation but with another coefficient. Henry [72] and Summer and Henry [182] in 1931 confirmed the Smoluchowski result.

For a potential with spherical symmetry Eq. (3.6) has the form

$$\frac{1}{r^2}\frac{d}{dr}\left(r^2\frac{d\Psi}{dr}\right) = \kappa^2\Psi. \tag{6.2}$$

Let the radius of particle be a and the potential on its surface Ψ_0. The solution of this equation, vanishing as $r \to \infty$, is

$$\psi = \Psi_0\left(\frac{a}{r}\right)\mathrm{e}^{-\kappa r}. \tag{6.3}$$

The charge on the particle q must balance that in the double layer

$$q = -\int_a^\infty \rho^e 4\pi r^2 dr.$$

From (3.2) and (6.2) we find

$$\rho^e = \varepsilon\varepsilon_0\kappa^2\Psi,$$

and

$$q = 4\pi\varepsilon\varepsilon_0 a(1+\kappa a)\Psi. \tag{6.4}$$

O'Brien and White [137] performed in 1978 the analysis of a model of electrophoresis which consists of a single charged colloid particle immersed in an electrolyte. The main physical idea used in the explanation of the system lies in that the electrical field of the particle causes the velocity of counterions first to increase as they approach the particle and then to decrease as they move downstream from the particle. These authors show that the Smoluchowski relation (6.1) holds for values of $\zeta \leq \mathcal{O}(1)$. For higher values the

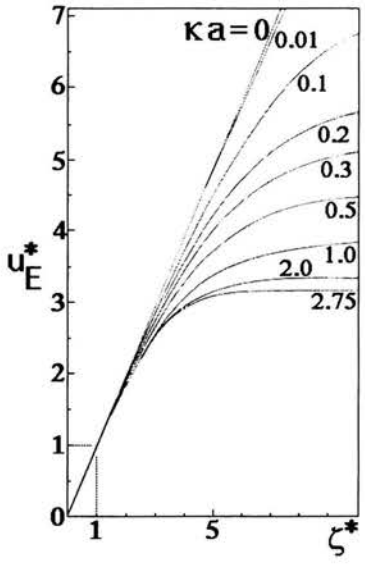

FIGURE 10. Reduced mobility u_E^* of a spherical colloid particle of radius a in a salt KCl solution as a function of reduced ζ^* potential, for $\kappa a \leq 2.75$. We observe that for small values of ζ^* the Smoluchowski relation (6.1) holds, for example $u_E^* = 1$ for $\zeta^* = 1$; after [137].

relation is nonlinear, as depicts Fig. 10, where the reduced mobility u_E^* and reduced ZP ζ^* were used

$$u_E^* = \eta \frac{1}{\varepsilon\varepsilon_0} \frac{\mathrm{e}}{\mathrm{k_B}T} u_E \quad \text{and} \quad \zeta^* = \frac{\mathrm{e}}{\mathrm{k_B}T}\zeta. \tag{6.5}$$

As Fig. 10 shows for values $\kappa a \leq 2.75$ the mobility increases with ZP in a monotonical manner. For $\kappa a \geq 3$ the mobility curves have maximum at $\zeta^* \approx 5$.

The above theory of electrophoresis deals only with one colloid particle and neglects its interactions with other colloid particles. The ability of electrolytes to flocculate various aqueous dispersions has been recognized already in the 19th century. However, only after development of the EDL theory, Derjaguin and Landau [33] in 1941 and Verwey and Overbeek [198] in 1948 could propose the theory of colloid stability (known as the DLVO theory).

Electrophoresis is often used to measure the average ZP on particles. However, in making predictions of colloid forces and stability, the distribution of ZP on the particles is important, cf. Fig. 11. Recently, Velegol [197] and Velegol *et al.* [196] demonstrated that since typical translational mobility measurements are much less sensitive to random charge nonuniformity than

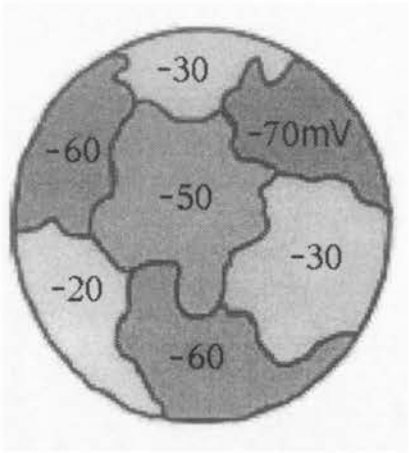

FIGURE 11. Nonuniform distribution of ZP on the surface of a sphere. Each patch has a different ZP (units mV), after Velegol *et al.* [196].

rotational mobility measurements, the latter measurement is more adequate for determining the second moment of the distribution of ZP.

7. Surface electrical potentials of plant cell membranes

As pointed out by Kinraide *et al.* [85] in 1998 the plasma membrane (PM) electrical phenomena play an important role in plant physiology, especially plant-mineral interactions. Two global electrical properties of the PM are distinguished. The first is the transmembrane electrical potential difference Ψ_m, which may be measured relatively easily by the insertion of a microelectrode into cells *in situ* (Nobel [134], Marschner [114]). The potential Ψ_m is responsive to many factors, including the composition of the bathing medium, the activity of ion pumps, and the state of ion channels, which are themselves responsive to Ψ_m (Hille [73]). The second global electrical feature of the PM is the electrical potential at the PM surface Ψ_0, the measurement of which is more difficult than the measurement of Ψ_m. The procedure entails the preparation of protoplasts or PM vesicles whose electrophoretic mobility is then measured to obtain a potential which reflects the electrical potential at the hydrodynamic plane of shear at a small distance from the PM surface (McLaughlin [117], Morel and Hering [124]). Consequently, the ZP has a somewhat lower magnitude than the Ψ_0. Only a few ZP measurements have been reported for the plant PM, see Table I in Kinraide *et al.* [85] and Obi *et al.* [135], Filek *et al.* [45].

Yermiyahu *et al.* [206] have developed in 1997 a model which takes into account the osmotic potential in the growing solution and the computed

amount of Ca^{2+} bound to the PM. Calcium binding was calculated by applying a Gouy-Chapman-Stern sorption model (see Section 3) using the same parameters deduced from the studies on PM vesicles. This model combines electrostatic theory with competitive binding at the PM surface. Kinraide *et al.* [85] have developed a Gouy-Chapman-Stern model for the computation of surface electrical potential Ψ_0 of plant cell membranes in response to ionic solutes.

8. Streaming potentials in cartilage

8.1. Components of cartilage

In articular cartilage a molecular origin of SP is observed. The main component of articular cartilage is the extracellular matrix which primarily consists of fixed negatively charged proteoglycan (aggrecan) chains kept by a collagen network, cf. Figs. 12 and 13. Both these constituents are hydrated with water containing mobile ions, cf. Maroudas [111], Mizrahi *et al.* [122], Mow and Ratcliffe [127]. Especially, in articles by Maroudas *et al.* [112] and [113] a two-compartment model of cartilage matrix was presented. The collagen network resists to extension and shear, while the proteoglycan resists to shear and compression, cf. Jin and Grodzinsky [83]. The latter is due to a high swelling pressure originating from electrostatic repulsion between adjacent glycosaminoglycan (GAG) chains, cf. Buschmann and Grodzinsky [19].

8.2. Generation of streaming potentials in cartilage

The low hydraulic permeability of cartilage (being a result of a very fine pore size) enables generation of high interstitial fluid pressure during loading, as indicated in 1976 Mansour and Mow [107]. Another consequence of fluid displacement with respect to collagen scaffold in the interstitium of loaded cartilage is generation of electric field or the SP. The electric potential appears due to the separation by fluid motion of negative charges, fixed to GAG chains, and positive charges dissolved in water, see Fig. 14.

Oscillatory compression of cartilage under physiological loads produces electrical potentials that are the result of an electrokinetic (streaming) transduction mechanism. Frank and Grodzinsky [48] observed in 1987 two additional electromechanical phenomena in the cartilage: streaming current and current-generated stress. Both these phenomena were found to be consistent with the same electrokinetic transduction mechanism responsible for the streaming potential. Changes in the measured streaming potential that

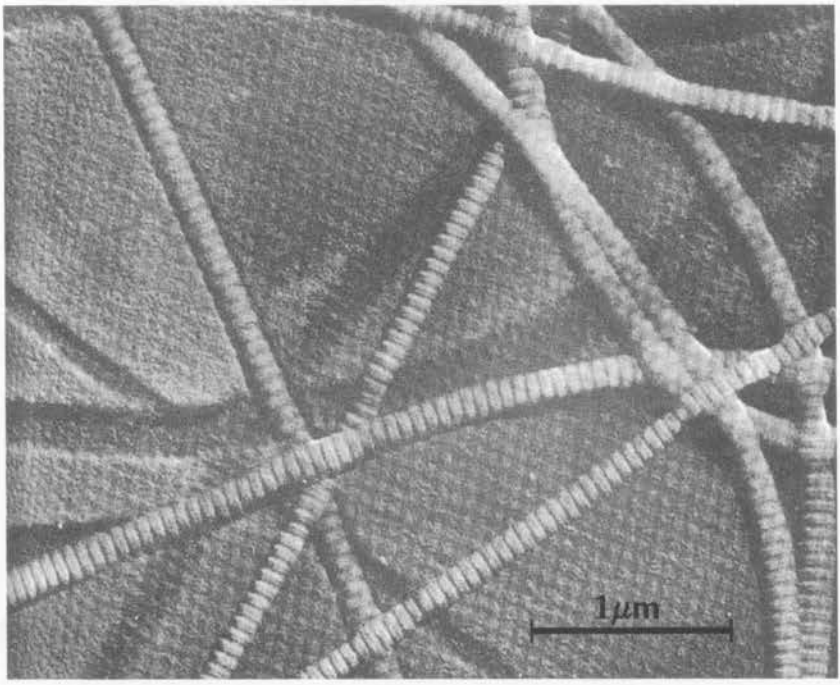

FIGURE 12. Electron micrograph of air-dried, chromium shadowed collagen fibrils from adult human corium; magnification × 26000, after Gross and Schmitt (1948) in: Harrington and von Hippel [69].

resulted from modification of bath ionic strength and pH provided additional insight into the molecular origins of these transduction processes. They also observed the SP in living cartilage maintained in organ culture, as well as in previously frozen tissue.

The SP was previously, in 1969, measured by Maroudas *et al.* [110] in confined compression using two electrodes. Recently, in 2002, thy SP was measured on the surface of the articular cartilage in uniaxial unconfined compression using a linear array of microelectrodes, see Garon *et al.* [53]. The apparatus for measuring SP is shown in Fig. 15. Potential profiles were obtained for sinusoidal and ramp/stress - relaxation displacements, and exhibited dependence on radial position, sinusoidal amplitude and frequency, time during stress relaxation, and on ionic strength. The measurements agreed with trends predicted by biphasic and related models, cf. [4], [84], [23], [175] and [102].

The absolute potential amplitude was maximal at the disk center, as was the predicted fluid pressure, and the electric field (the potential gradient) was maximal at the disk periphery, as was the predicted fluid velocity.

FIGURE 13. Aggrecan molecules of length of about 450nm, after Ng *et al.* [130].

After correcting for the effect of filters the radial SP profiles were constructed by addition of the differential profiles across the radius, see Fig. 16.

8.3. Regulation of cartilage activity

The function of articular cartilage is maintained by chondrocytes *via* degradation and synthesis of extracellular matrix constituents, cf. [70]. While tissue culture experiments have convicingly characterized the sensitivity of cartilage for mechanical stimuli, the cellular-level physical signal that chondrocytes sense an to which they respond remains unclear, [36]. *In vivo* compression of cartilage results in electrokinetic effects, hydrostatic pressure, direct cellular deformation and fluid flow, cf. [126]. It was demonstrated that chondrocytes respond to fluid flow among others with increases in intercellular calcium concentration ($[Ca^{2+}]_i$), prostoglandin E_2 release and proteoglycan synthesis, cf. [170], [204], [205].

Cellular metabolic activities are regulated by both genetic and environmental factors. For chondrocytes, it was demonstrated that these factors include deformations, fluid shear stress, hydrostatic and osmotic pressures, electrical potentials and currents. For example, cyclic strain induces alignment of chondrocytes perpendicular to the strain vector (Fig. 17c). Cells appear to be elongated and to have localized at the area of maximum strain,

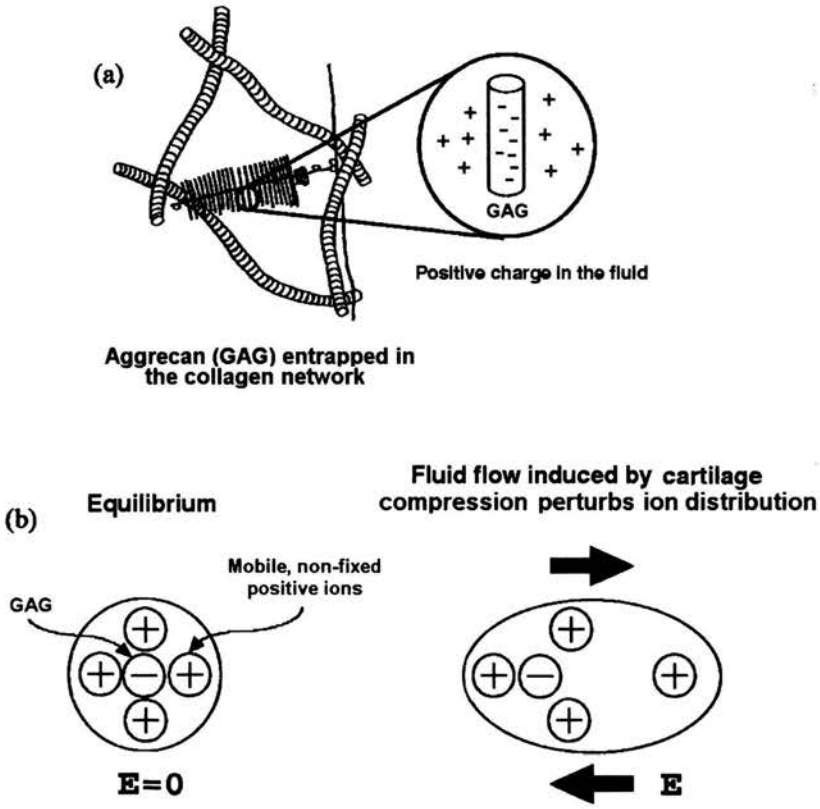

FIGURE 14. Molecular origin of streaming potential in cartilage. (a) The aggrecan (GAG) is kept by the collagen network. A large number of ions with negative charges is deposed on GAG chains. Clouds of mobile positive ions surrounds the fixed GAG negative charges and neutralizes its. (b) Fluid flow seperates positive from negative ions and creates an electric field **E**, after Garon *et al.* [53].

i.e., toward the edge of the plate. Flexed cells produce a darker shade, indicating that there is an increase in protein expression for collagen type II (Fig. 17c,d). We observe that swelling of the articular cartilage, it depends on its fixed charge density (FCD) and distribution, the stiffness of its collagen-proteoglycan matrix, and the ion concentrations in the interstitium.

Frank and Grodzinsky [47] indicated in 1983 that SPs are a sensitive index of articular cartilage degeneration. Later Frank *et al* [50] observed significant changes in the potential response due to chemical modifications of the matrix. Simultaneously, Frank and Grodzinsky [49] formulated a continuum model for linear electrokinetic transduction in cartilage. The formulae were derived for the SP induced by oscillatory, uniaxial confined compression of the tissue

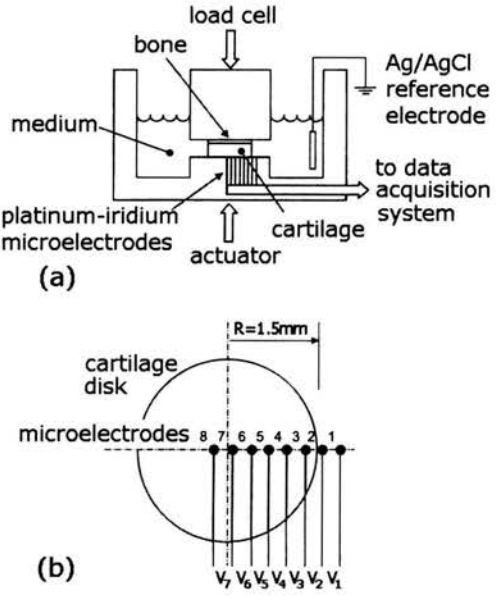

FIGURE 15. Experimental apparatus for spatial resolved detection of streaming potentials. (a) Full thickness cartilage disks were compressed in a saline bath under uniaxial unconfined compression. (b) The flow induced electric fields (streaming potentials) were merasured across the radius of disk *via* a linear array of 8 electrodes embedded in the base of testing chamber; after Garon *et al.* [53].

as well as the mechanical stress generated by a current density or potential difference applied to the tissue. The experimentally observed streaming potential and current-generated stress response were compared with the predictions of the theory over a wide frequency range. The theory coincides well with the data for reasonable values of cartilage intrinsic mechanical parameters and the electrokinetic coupling coefficients. Experiments also show a linear relationship between the stimulus amplitude and the transduction response amplitude, within the range of stimulus amplitudes of interest.

To describe the deformation and stress fields for cartilage under chemical and mechanical loads, Lai *et al.* [92] have proposed in 1991 a theory for a tertiary mixture, including the two fluid-solid phases (biphasic), and an ion phase, representing cation and anion of a single salt. This triphasic theory combines the physico-chemical theory for ionic and polyionic (proteoglycan) solutions with the biphasic theory for cartilage. The model assumed the fixed charge groups to remain unchanged, and that the counter-ions are the cations of a single salt of the bathing solution. The momentum equation for the neutral salt and for the interstitial water are expressed in terms of their chemical

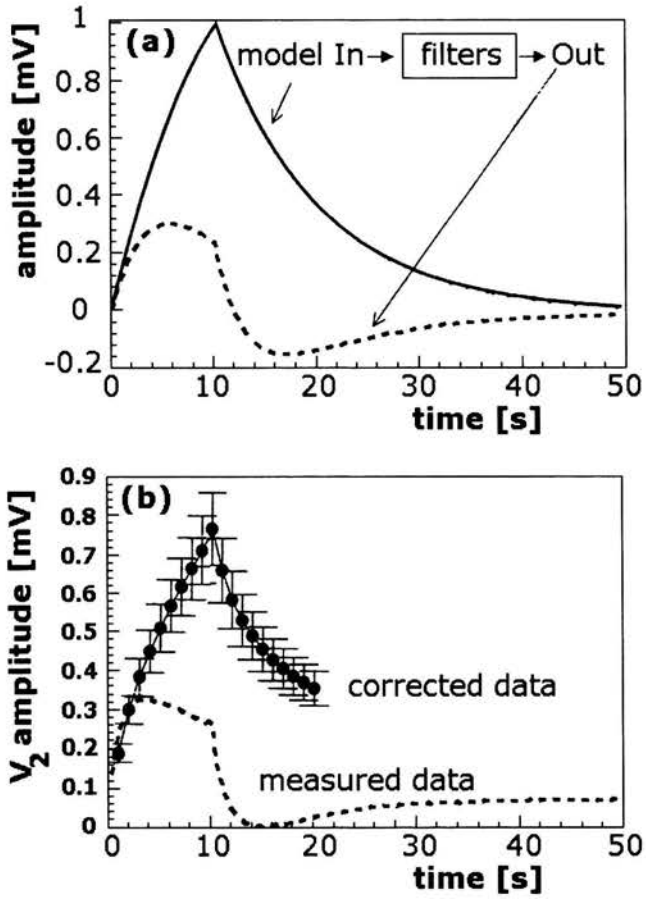

FIGURE 16. Streaming potentials measured during stress relaxation. Streaming potentials were acquired during ramp rise and subsequent stress relaxation. (a) The theoretical effect of the high- and low-pass filters (cut-off frequencies of 0.05 and 200Hz, respectively) on a typical stress-relaxation signal. (b) Corrected differential signals, after processing of acquired data, using an experimentally determined transfer function for the filter effects; after Garon *et al.* [53].

potentials whose gradients are the driving forces for their movements. This theory was applied to both equilibrium and non-equilibrium problems, and was later often applied and developed, especially as a quadriphasic theory, see [80], [81] and the references therein.

Next, in 1993 Gu *et al.* [62] using the triphasic mechano-electrochemical theory of Lai *et al.* [92] analyzed the transport of water and ions through a finite-thickness layer of charged, hydrated soft tissue (articular cartilage) in one-dimensional steady permeation experiment. They obtained in numerical

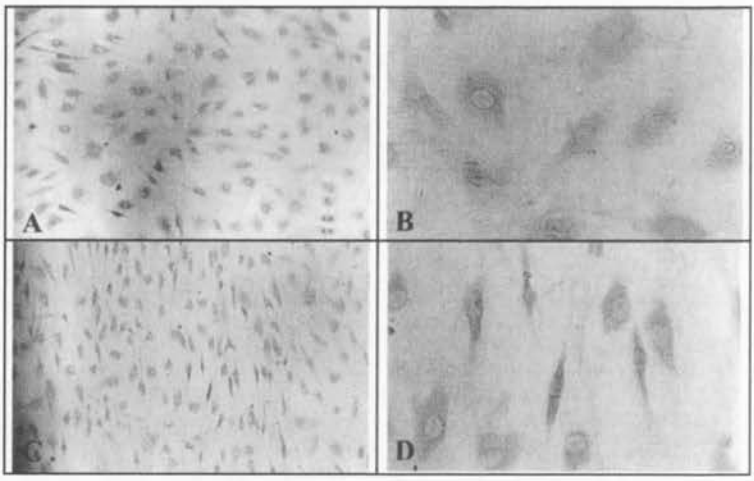

FIGURE 17. Micrographs of immunostained chondrocytes subjected to static or to cyclic strain. (a) Chondrocytes kept in static condition (original magnification 100×); (b) chondrocytes kept in static condition (400×); (c) chondrocytes subjected to flex-cyclic strain (100×); (d) chondrocytes subjected to flex-cyclic strain (400×); after Lahiji *et al.* [96].

way the concentrations of the ions, the strain field and the fluid and ion velocities inside the specimen subject to an applied mechanical pressure and osmotic pressure across the layer. The relationships giving the dependence of the SP and permeability on the negative FCD of the tissue were derived analytically for the linear case, and calculated for the nonlinear case. Among the results obtained were: (1) at the fluid pressure difference of 0.1 MPa across the specimen layer, there is a 10% flow-induced compaction at the downstream boundary; (2) the flow-induced compaction causes the FCD to increase and the neutral salt concentration to decrease in the downstream direction; (3) while both ions move downstream, relative to the solvent (water), the anions Cl^- move with the flow whereas cations Na^+ move against the flow. The difference in ion velocities depends on the FCD, and this difference attained a maximum at a physiological FCD of around 0.2 meq/ml; (4) the apparent permeability decreases nonlinearly with FCD, and the apparent stiffness of the tissue increases with FCD; and (5) the SP is not a monotonic function of the FCD and it has a maximum value within the physiological range of FCD for articular cartilage. The experimental data on SP obtained from bovine femoral cartilage support the triphasic theoretical prediction of non-monotonicity of the SP as a function of the FCD.

Chen *et al.* [21] determined in 2001 the depth-varying confined and osmotic compression moduli of normal human articular cartilage from the fe-

moral head, and tested whether these moduli are dependent on FCD. Using an automated instrument to allow epifluorescence microscopy analysis during confined compression testing on cartilage samples, the equilibrium confined compression modulus was found to vary markedly with depth (0-1500 μm) from the articular surface. The confined compression modulus of normal aged human femoral head articular cartilage increases markedly with depth from the articular surface. The compressive properties are not simply related to FCD at different depths from the articular surface, as in Gu *et al.* [62], suggesting that other yet undefined factors contribute to compressive properties.

Gu *et al.* [63] proposed in 1998 a new mixture theory to model the mechanical and electrochemical behaviour of charged and hydrated soft tissues containing multi-electrolytes. The mixture is composed of $2+n$ constituents (1 charged solid phase, 1 noncharged solvent phase, and n ion species). Results from this theory show that 3 types of force are involved in the transport of ions and solvent through such materials: (1) a mechanochemical force (including hydraulic and osmotic pressures), (2) an electrochemical force; and (3) an electrical force. The results obtained also show that 3 types of material coefficients are required to characterize the transport rates of these ions and solvent: (1) the hydraulic permeability, (2) the mechano-electrochemical coupling coefficients; and (3) the ionic conductance matrix. The relationships between these forces and the material coefficients describing such mechano-electrochemical transduction effects as the streaming potential, streaming current, diffusion (membrane) potential, electro-osmosis, and anomalous (negative) osmosis were derived. The authors showed that the Hodgkin-Huxley formula from 1952 for the resting cell membrane potential could be derived using their mixture model, cf. [74]. Numerical results were provided for the exchange of Na^+ and Ca^{2+} through the cartilage. These numerical results support the hypothesis that tissue FCD plays a significant role in modulating kinetics of ions and solvent transport through charged-hydrated soft tissues.

Earlier, a description of such processes was elaborated by us, not on the basis of solid-liquid mixture theories, but by using homogenisation methods. In this description the cartilage was approximated as a periodic porous medium [188], [203], cf. also [52]. On the solid-liquid interfaces all necessary conditions for mechanical and electrical variables were satisfied.

The sequence of events involved in the transduction of mechanical signals to a biochemical signal is not fully understood. Guilak *et al.* [67], claim that an increase in the concentration of intracellular calcium ion $[Ca^{2+}]_i$ is one of the earliest events in the process of cellular mechanical signal transduction. With use of fluorescent confocal microscopy, $[Ca^{2+}]_i$ was monitored in isolated articular chondrocytes subjected to controlled deformation with the edge of a glass micropipette. Mechanical stimulation resulted in an immedia-

te and transient increase in $[Ca^{2+}]_i$. The initiation of Ca^{2+} waves was abolished by removing Ca^{2+} from the extracellular media and was significantly inhibited by the presence of gadolinium ion (10 μM) or amiloride (1 mM), which block mechanosensitive ion channels. These findings suggest that a possible mechanism of Ca^{2+} mobilization in this case is a self-reinforcing influx of Ca^{2+} from the extracellular media, initiated by a Ca^{2+}-permeable mechanosensitive ion channel. Therefore, a transient increase in intracellular Ca^{2+} concentration may be one of the earliest events involved in the response of chondrocytes to mechanical stress and support the hypothesis that deformation-induced Ca^{2+} waves are initiated through mechanosensitive ion channels, see also [148]. It is therefore a possible way in which chondrocytes utilize mechanical signals from their environment to regulate metabolic activity of articular cartilage.

Lai *et al.* [93]-[95] investigated the nature of the electric field inside articular cartilage while accounting for the effects of both *streaming potential* and diffusion potential. Using the triphasic theories they solved two tissue mechano-electrochemical problems: (1) the steady 1D permeation problem, and (2) the transient 1D ramped-displacement, confined-compression, stress-relaxation problem (both in open circuit condition). Calculations showed that in these two cases the diffusion potential effects compete with streaming potential for dominance of the electric potential inside the tissue. For softer tissues of similar FCD, the diffusion potential effects are enhanced when the tissue is being compressed (i.e., increasing its FCD in a nonuniform manner) either by direct compression or by drag-induced compaction; the diffusion potential effect may even dominate over the streaming potential effect. The polarity of the electric potential field is in the same direction of interstitial fluid flow when the SPs dominate, and in the opposite direction of fluid flow when diffusion potential dominates.

8.4. Experimental investigations of cartilage properties

Schneiderman *et al.* [169] studied in 1986 the effects of mechanical and osmotic compression on sulphate incorporation into glycosaminoglycans of human femoral head cartilage. They found that both mechanical and osmotic compression produce the same lowering of sulphate uptake relative to uncompressed controls. It appears that this effect is not associated with changes in solute transport or changes in solute concentration in the matrix, but is due, in part at least, to an increased osmotic pressure acting on the chondrocytes. A second mechanism might be involved directly through the increased proteoglycan concentration in the pericellular environment, resulting from a reduction in the water content. They also found that glycosaminoglycan

synthesis returned to its control level when the conditions prevailing in the matrix, in the absence of pressure or added solute, were restored.

Guilak *et al.* [66] investigated in 1994 the effects of compressive stress on the rate of proteoglycan synthesis and release in bovine articular cartilage from 4-5-month-old animals. Full depth cartilage explants were compressed in an unconfined configuration at various stresses ranging up to 1.0 MPa. While cartilage composition and biosynthetic activity were found to vary significantly with depth in control cartilage, the observed suppression (% change) in biosynthetic activity was relatively uniform with depth in both loading and recovery experiments. The study seemed to indicate that compression of the tissue to physiological strain magnitudes serves as a signal to modulate the chondrocyte biosynthetic and catabolic response through the depth of cartilage, while prolonged compression at higher strains might be responsible for tissue and cell damage.

The effects of the SP, fluid flow and hydrostatic pressure on chondrocyte biosynthesis were studied in 1995 by Young-Jo Kim *et al.* [209]. Those authors compared the spatial profiles of these physical stimuli to the profiles of biosynthesis within cartilage disks subjected to dynamic unconfined compression. The radial SP was measured using compression frequencies and disk sizes relevant to studies of physical modulation of cartilage metabolism; a general analytical solution to the unconfined compression of a poroelastic cylinder with impermeable, rigid, adhesive platens was derived using potential theory. The solution with adhesive platen boundary conditions, using measured values of cartilage material properties, predicted SPs that were much closer to experimental results betwen 0.001 and 1 Hz than a solution using frictionless platen boundary conditions. The predicted radial profiles of SP gradient and fluid velocity (but not hydrostatic pressure) were similar to the previously reported on radial dependence of proteoglycan synthesis induced by dynamic unconfined compression.

Bonassar *et al.* [16] investigated in 1996 activation and inhibition of endogenous matrix metalloproteinases in articular cartilage, and its effects on composition and biophysical properties of cartilage. Bovine cartilage explants were cultured with 1 mM 4-aminophenylmercuric acetate (APMA) to activate endogenous matrix metalloproteinases (MMPs). Additionally, graded levels of either rhTIMP-1 (recombinant human tissue inhibitor of metalloproteinases-1) or L-696-418 (a synthetic metalloproteinase inhibitor) were used to inhibit degradation induced by APMA. Treatment with APMA resulted in as much as 80% loss in the tissue GAG content, a greater than threefold increase in denatured type II collagen as determined by the presence of CB11B epitope, and complete loss of biosynthetic activity after 3 days in culture. The inhibition of APMA-induced GAG loss by 4μM TIMP

was accompanied by maintenance of the *streaming potential*, electrokinetic coupling coefficient and dynamic stiffness.

Probably the first data for the SP of human intervertebral disc tissues were reported in 1999 by Gu *et al.* [64]. In order to investigate the influence of the changes in tissue structure and composition on the electrokinetic behavior of intervertebral disc tissues, those authors measured the SP response of non-degenerate and degenerate human *annulus fibrosus* (AF) in a one-dimensional permeation configuration under static and dynamic loadings. It was found that the static SP of the AF depended on the degenerative grade of the discs and on the specimen orientation in which the fluid flows. For a statically applied pressure of 0.07 MPa, the ratio of SP to applied pressure ranged from 5.3 to 6.9 mV/MPa and was the largest for tissue with axial orientation and the lowest for tissue with circumferential orientation. The alteration of SP reflects the changes in tissue composition and structure with degeneration. In such a manner the knowledge of the SP response of the intervertebral disc facilitates an understanding of signal transduction mechanisms in the disc and the etiology of intervertebral disc degeneration.

8.5. Mixture theory applied to the description of cartilage

Recent (2003) appplication of the mixture theory is due to Ateshian *et al.* [5] in their study of cartilage lubrication, cf. also van Meerveld and Huyghe [118], van Meerveld *et al.* [119]. It was assumed that each phase of the mixture (solid matrix, water, cations and anions) is incompressible and the mixture is saturated. Only one cation and one anion species of equal valence are considered. The continuity equation is

$$\nabla \cdot \mathbf{v}^s + \nabla \cdot \left[\sum_{\beta=w,+,-} \varphi^\beta (\mathbf{v}^\beta - \mathbf{v}^s) \right] = 0 \tag{8.1}$$

where $\mathbf{v}^s$ is the solid matrix velocity, $\mathbf{v}^\beta$ are the water solvent ($\beta = w$) and ion velocities ($\beta = +, -$), and φ^β are their corresponding volumetric fractions. For an infinitesimal strain $\mathbf{e}$ and $\varphi^+, \varphi^- \ll 1$, the mixture saturation condition $\sum_{\beta=s,w,+,-} \varphi^\beta = 1$ leads to the relation

$$\varphi^w = \frac{\operatorname{tr}\mathbf{e} + \varphi^w_\infty}{\operatorname{tr}\mathbf{e} + 1} \approx \varphi^w_\infty + (1 - \varphi^w_\infty) \operatorname{tr}\mathbf{e} \tag{8.2}$$

where φ^w_∞ is the water volume fraction when the cartilage is in hypertonic solution, for which $\mathbf{e} = \mathbf{0}$. Since the proteoglycans are fixed to the solid matrix, their FCD is given by c^F and has then the form

$$c^F = c^F_\infty \frac{\varphi^w_\infty}{\operatorname{tr}\mathbf{e} + 1} \approx c^F_\infty \frac{1 - \operatorname{tr}\mathbf{e}}{\varphi^w_\infty}. \tag{8.3}$$

The momentum equations for the water solvent ($\alpha = w$) and each of the ions constituents ($\alpha = +, -$) are given by

$$\rho^\alpha \nabla \mu^\alpha + \sum_{\beta=s,w,+,-} f_{\alpha\beta}(\mathbf{v}^\beta - \mathbf{v}^s) = \mathbf{0}, \tag{8.4}$$

where μ^α is the electrochemical potential of the α constituent (unit J/kg) and $f_{\alpha\beta}$ (N s/m^4) is the frictional coefficient between α and β constituents (with $f_{\alpha\beta} = f_{\beta\alpha}$ and $f_{\alpha\beta} = 0$ when $\alpha = \beta$). The apparent density ρ^α (kg/m^3) of each ion constituent is related to its concentration c_α (mol/m^3 of solvent) and molecular mass M_α (kg/mol) through $\rho^\alpha = \varphi^w M_\alpha c_\alpha$, while for the water solvent $\rho^w = \varphi^w \rho_T^w$ where ρ_T^w is the true solvent density. The momentum equation for the whole mixture (solid + solvent + 2 ion species) is given by

$$\nabla \cdot \mathbf{s} = \mathbf{0}, \tag{8.5}$$

where $\mathbf{s}$ is the total mixture stress. The electroneutrality of the mixture is expressed by

$$\sum_{\alpha=+,-} z_\alpha c_\alpha - c^F = 0, \tag{8.6}$$

where z_α is the algebraic valence of the α ionic species ($z_+ = +1$, $z_- = -1$). In the absence of electrical current in the tissue (open-circuit) the following relation for the current density holds

$$I_c = \mathrm{F}_c \varphi^w \sum_{\alpha=w,+,-} z_\alpha c_\alpha (\mathbf{v}^\alpha - \mathbf{v}^s) = \mathbf{0} \tag{8.7}$$

where F_c is the Faraday constant. The model is completed by constitutive relation for the stress and chemical potential. Soltz and Ateshian [174] demonstrated that conewise linear elasticity of Curnier *et al.* [29] together with the biphasic mixture theory provide a model of cartilage consistent with reports in the literature.

The mixture theory appeared useful for modelling of different aspects of bone behaviour. Molenaar *et al.* [123] treated the bone as a composite of four constituents: porous solid matrix (s), compressible fluid (f), cations (+) and anions (−). Charged porous medium is described by Hooke's law in which an effective stress is involved.

It seems that until now the electrokinetic theories proposed for AC have not been incorporated into electromechanical modelling of cartilage and other biological materials. We mean here application of the theories presented in Section 5.1.

9. Electromechanical behaviour of wet collagen

The electrical behaviour of collagen molecules was studied in 1968 by Anderson and Eriksson [3] on an example of a specimen prepared from the human Achilles tendon. This tendon consists of collagen fibres, largely parallel to the long axis of tendon, which typically was 5cm long and 8mm in diameter. Because of this structure there is a large number of fine capillary channels throughout the length of the specimen, through which liquid can flow. When tendon is stretched, liquid is squeezed out and flows into the specimen when it is relaxed. Such movement of ionic fluid gives rise to streaming potentials.

The essential characteristic used in their experiment was the concept of isoelectric point which determines the condition (pH level) at which ampholytic molecules or particles have no electrophoretic mobility. When ZP is just zero, the particle do not migrate at all in the electric field; it is said to be the isoelectric point. The isoelectric point is expressed in pH units. Various ampholytes, such as proteins, have their isoelectric point somewhere between pH 4 and 10. The isoelectric point of predominatly acid ampholytes is at low pH, while predominatly basic ampholytes have these points at pH values higher than 7.

9.1. Role of moisture in the collagen structure

Collagen molecules are structural macromolecules of the extracellular matrix. The works by Esipova *et al.* [40] performed on rat tail tendon (RTT) samples in 1958 indicated that the water molecules do modify the collagen chain.

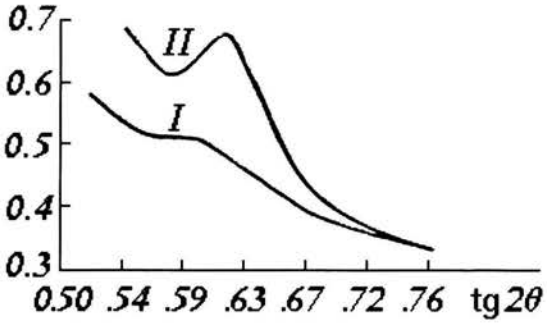

FIGURE 18. The intensity of X ray interference for two moisture contents in RTT collagen samples: I - dried sample, II - sample with 81% of moisture; θ is scattering angle, after Esipova *et al.* [40].

In order to determine the specific role of water in the structure of collagen, these authors investigated changes of the intensity of collagen X-ray reflection with respect to the water content in the collagen. Experimental data demonstrated that the intensity of *crystalline reflections* decreased uniformly in response to the decrease of the water content in the samples, see Fig. 18. The amorphous ring appeared at the same time. This suggests that the water molecules stabilise in some way the crystalline structure.

9.2. Experimental separation of streaming and piezoelectric potentials

Anderson and Eriksson [3] carried out an experiment in which the SPs could be separated from any piezoelectric potential that might be present. In order to separate the two effects, the tendon specimen should be strained and the potential developed between two electrodes buried into it measured, with the *p*H of the surrounding solution varied through the isoelectric point. If the potentials were observed at the normal isoelectric *p*H for collagen they would be attributed to piezoelectric effects.

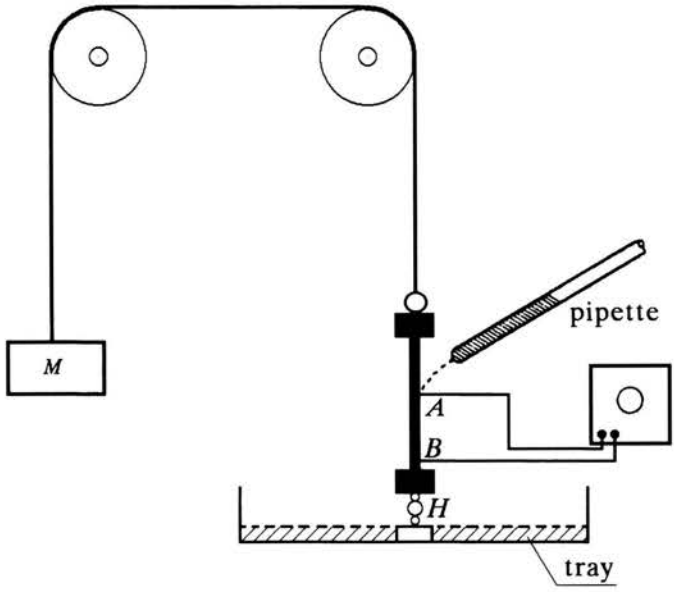

FIGURE 19. Diagram of the apparatus used for separation of streaming and piezoelectric potential, after Anderson and Eriksson [3].

The diagram of the apparatus is shown in Fig. 19. The tendon specimen was anchored to a brass hook H by means of a stainless steel wire suture at

the lower end. The upper end was attached to piano wire, also by stainless steel wire, which passed over two pulleys and was attached to the mass M. In points A and B, Ag-AgCl electrodes were buried into the tendon, 3 cm apart, by injecting them through a fine capillary tube and subsequently withdrawing the tube. The leads from the the electrodes were taken to an ocislloscope with a storage screen. The tendon was prepared by allowing it to dry in a desiccator at room temperature until it was stiff and brittle. It was then immersed in a solution of known pH, prepared from standard buffer solution. To obtain readings a standard impulse was applied to the specimen by allowing the mass M, 2 - 10kg, to fall through a fixed distance of 1 in. The resulting electrical pulse was displayed on the oscilloscope.

According to the idea of SPs the signal obtained was proportional to the load and at pH 4.7 no signal was obtained whatever the force applied. This means that no piezoelectric effect was manifested. A graph of the peak value of voltage pulse against pH of the solution is shown in Fig. 20.

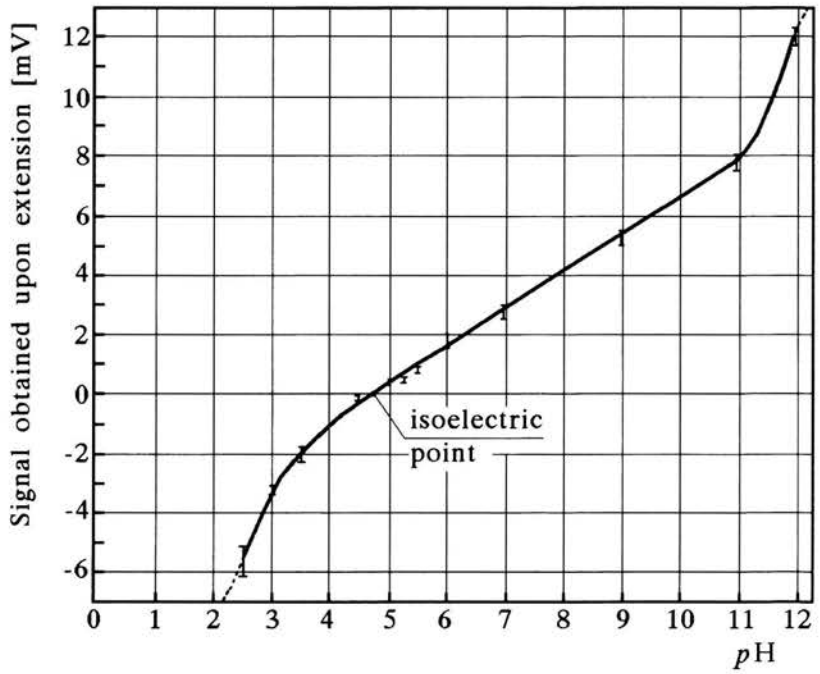

FIGURE 20. The peak value of the voltage pulse as a function of pH of the solution, after [3].

9.3. Isoelectric point for human Achilles tendon

The tendon was dried and ground up, using fine glass paper and a homogenizer. The mean particle size was estimated to be of 20μm, and specimen solutions were made up by adding powder to to the recommended buffer solutions for electrophoresis, covering the range of pH values from 3.5 to 10.

The electrophoretic velocity of particles with a current of 5 mA passing through the solution cell is plotted against pH in Fig. 21 for an ionic strength of 0.05M. Because an applied electric field has no effect on the particles at a pH value of 4.7, this is taken to be the isoelectric point for the human Achilles tendon.

As the isoelectric point is the condition (pH value) at which the ZP becomes zero, the coincidence of the isoelectric point with pH for zero electrical impulse potential indicates that the impulse potentials involved are caused by SPs only, there being no contribution from the piezoelectric effect. It is therefore concluded that the piezoelectric effect is not observed in the completely wet collagen.

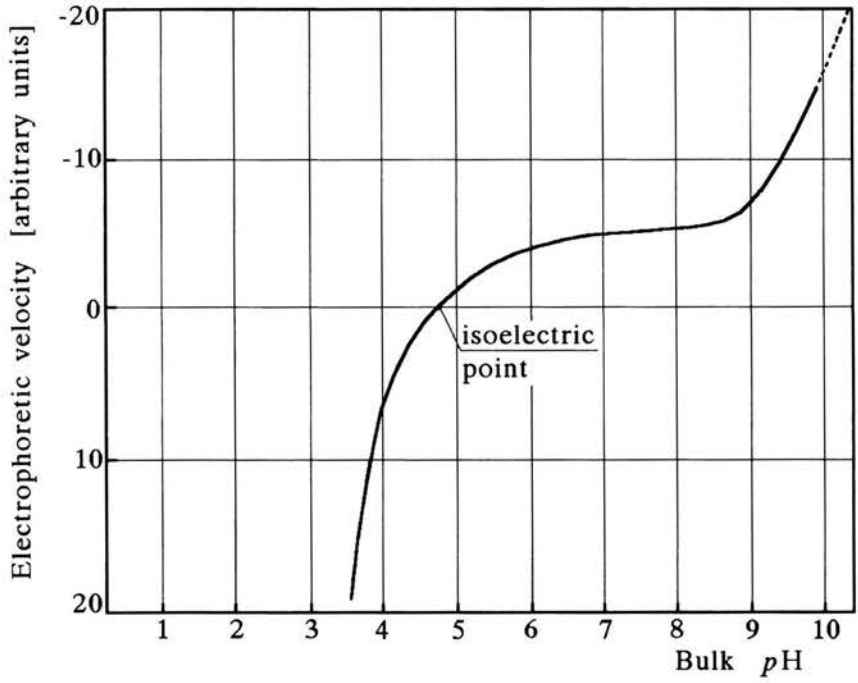

FIGURE 21. The electrophoretic velocity of tendon particles, with a current of passing through the cell, as a function of pH, after [3].

As it was noted in the previous section, the experiments by Esipova *et al.* [40] indicated that the water molecules do modify the collagen chain in such a way that the intensity of collagen X-ray reflection with respect to water content in collagen increases with the increase of water content and the amorphous ring disappears at the same time. Thus the moisture enhances crystallographic properties of collagen. It seems that there is no reason to assume that the piezoelectric effect does not exist in wet collagen. However, it rests hidden by the conditions of experiment - because of high dielectric and conductive properties of electrolyte. It is not clear, if the piezoelectric effect could be manifested locally, in a region of collagen itself, and if it could influence the action of chondrocyte distributed nearby.

Tissue collagen exhibits several levels of structural organization, and this complicates efforts to determine the origin of its piezoelectricity. Marino *et al.* [109] made in 1980 collagen films - by evaporation and electrodeposition from solution- and examined the relation between the collagen piezoelectricity and its electron microscopic appearance. They found that the electrodeposited films were more organized and exhibited higher piezoelectric coefficients than the evaporated films. Despite this, the evaporated films were piezoelectric, thereby suggesting that the effect originates either at the level of the tropocollagen molecule or, at most, is linked with aggregated structures no larger than 50Å in diameter.

10. SPs in mechanosensory system in bone

Bone is a tissue containing a fluid phase, a porous solid matrix, and cells. Movement of the fluid phase within the pores or spaces of the solid matrix translates endogenous and exogenous mechanobiological, biochemical and electromechanical signals to the cells that remodel the bone tissue, cf. review by Knothe Tate [91]. For more details on the topic the reader is referred to paper by Cowin in this volume. Here only some experiments related to the role of SPs for mechanosensory system in bone will be treated.

The skeleton ability to withstand extreme of physical activities is achieved in large part by its capacity to perceive and respond to small changes in its mechanical environment. Strains generated by functional activity represent an epigenetic parameter by which the bone cell population could assess the skeleton structural effectiveness, and subsequently influence its morphology. Rubin *et al.* [161] noted in 1990 that minimizing strain does not appear to be the paramount goal of adaptation, but rather the conditions under which the skeletal morphology interacts with functional activity to generate a certain, beneficial from cytological point of view, type of strain. Three levels are considered to address the influence of external loading on bone morphology: (a) the level of the organ, the strains generated by functional activity; (b)

the level of the tissue, osteoregulatory parameters of the strain environment; and (c) the level of the cell, the mechanisms by which physical information is translated to an adaptive response.

At the cellular level, Piekarski and Munro [143] showed in 1977 that cyclic loading, as naturally occurring in long bones, produces a flow of liquid through canaliculi of Haversian bone. Salzstein *et al.* [166], [167] remarked in 1987 that flow of fluid over the cell surface subjects the cell to two types of stimuli, fluid-induced drag forces (or fluid shear stress) and streaming electrical potentials. When compact bone is subjected to bending loads, interstitial fluid in the bone matrix flows away from regions of high compressive stress and the amount of interstitial fluid flow is strongly influenced by the loading rate.

The experimental proof of this phenomenon was provided recently by Knothe Tate *et al.* [89], [90] and Steck *et al.* [179]. Using low- and high-molecular-weight tracers, these authors studied the diffusive transport as well as the convective transport resulting from load-induced fluid flow in intact bones. They found that diffusion alone is not efficient for transport in the canaliculi of large molecules such as microperoxidase and that load-induced fluid displacements are necessary for maintenance of metabolic activity in osteocytes and activation or suppression of modelling processes.

The role of osteocytes as mechanosensors seems to be well established. *In vivo*, osteocytes have been shown to express mRNA for β-actin, osteocalcin, connexin-43, insulin-like growth factor I, cf. Mason *et al.* [115]. *In vitro*, osteocyte cultures were found to reestablish their stellate morphology and again form a network by cell processes and gap junctions (Nijweide and Mulder [131], Tanaka *et al.* [187], Van der Plas and Nijweide [195]), see Fig. 22.

While searching for a membrane mechanism for adaptation of bone to mechanical loading, stretch-activated channels in the chick osteoclasts were found. Ypey *et al.* [210] investigated in 1992 embryonic chick bone cells which express various types of ionic channels in their plasma membranes for as yet unresolved functions. Chick osteoclasts (OCL) have a rich variety of channel types. Specific for the OCL is a K^+ channel, which activates (opens) when the inside negative membrane potential becomes more negative. Other investigators found stretch-activated cation channels K^+ in rat and human osteogenic cell lines. These researchers did not find any of the classic macroscopic voltage-activated calcium conductances in any of the chick bone cells under the experimental conditions. However, the fluorescence measurements of $[Ca^{2+}]_i$ in single cells indicate the presence of Ca^{2+} conductive pathways through the plasma membrane of osteoblastic cells and osteoclasts.

Cowin *et al.* [25], Turner *et al.* [192] and Weinbaum *et al.* [199] hypothesized about 1995 that interstitial fluid flow affects bone formation, and tested

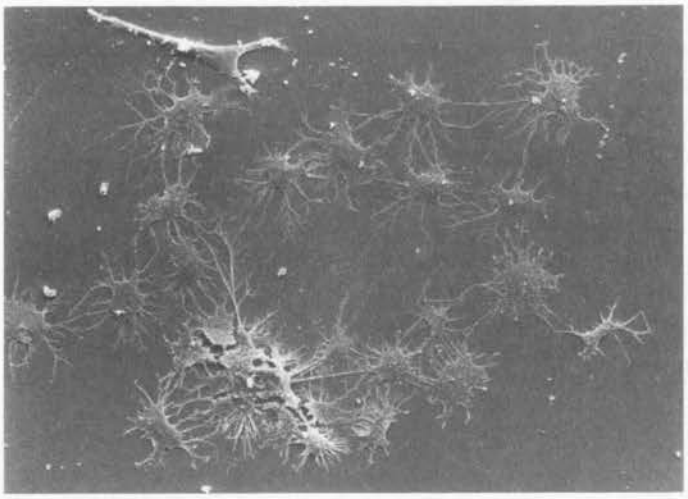

FIGURE 22. Scanning electron micrograph of a group of osteocytes, isolated from embryonic chicken calvariae, after 3 days of culture as monolayer. The cells have re-established a cellular network by moving away from each other and making thin, branching cell processes that connect with those of neighboring cells. The non-random distribution of the cell processes, and their straightness, suggest that the processes have a means to sense each other's presence. The cell in the upper left corner is a contaminating osteoblast. Micrograph by P. J. Nijweide, after Burger and Klein-Nulend [18]; cf. also [132].

this hypothesis indirectly by measuring the effect of different loading frequencies on bone formation rate *in vivo*. In a separate experiment, they found stress-generated potentials (SGPs) in the rat tibia to increase monotonically with increasing loading frequency. The dose-response relationship between loading frequency and the bone formation response closely resembles the relationship between loading frequency and the SGPs within the bone. The qualitative similarity between these two relationships suggests that increased bone formation is associated with increased SGPs which are caused by the interstitial fluid flow. Bone cells are known to be sensitive to electric fields and may respond directly to SGPs. Also, fluid shear forces have been shown to stimulate bone cells in culture, so it seems possible that increased interstitial fluid flow directly affects bone formation.

However, a later study found no effect of applying an external current, which either doubled or cancelled the convective current density, on the calcium response of bone cells to fluid flow. More precisely, Hung *et al.* [77], [78] performed in 1996 an experiment in which cultured bone cells subjected to fluid flow were exposed to mechanical forces and electrokinetic forces. The convective current establishes an electrokinetic force created by the flow-

dependent transport of mobile ions over the charged cell surfaces. This current can be expressed as a current density, the current normalized by the cross-sectional area in which it exists. It was shown that the convective current density has no role in the bone cell real-time intracellular calcium response to fluid flow. This result was tested by incorporating electrokinetic measurements and classical electrokinetic double-layer theory to estimate the value of convective current density in a parallel-plate flow chamber. Next, an external current was applied during the presence of fluid flow that would alter convective current density. There was no difference between the mean peak calcium response of cells exposed to flow with an altered (cancelled or doubled) convective current density *versus* flow with an unmodified convective current density. These data suggest that the fluid-induced shear stress, the direct mechanical perturbance of the cell (membrane), is the stimulus that conveys the mechanical message to the bone cell, in line with an earlier (1990) experimental study by Reich *et al.* [151].

Recently, to explore the hypothesis that load-induced fluid flow in bone is a mechano-transduction mechanism in bone adaptation, Swan *et al.* [184] used unit cell micro-mechanical techniques to relate the microstructure of the Haversian cortical bone to its effective poroelastic properties. Computational poroelastic models were applied to compute *in vitro* Haversian fluid flows in a prismatic specimen of cortical bone during harmonic bending excitations over the frequency range of 10^0 to 10^6Hz. Peak bone fluid pressures were found to increase linearly with the loading frequency, proportionally to peak bone stress up to frequencies of approximately 10 kHz. Haversian fluid shear stresses were found to increase linearly with excitation frequency and loading magnitude up until the breakdown of Poiseuille flow. The computational models indicate that fluid shear stresses and fluid pressures in the Haversian system could, under physiological loading, reach the level of a few Pascals, which were shown in other works to elicit cell responses *in vitro*.

10.1. Role of collagen in production of streaming potentials

In 1982 Gross and Williams [60] showed in direct streaming experiments that the potential expression (5.8) which was originally derived for a narrow cylindrical channel of uniform radius, describes correctly the dependence of the SPs on solution parameters for a disc of bone.

The SPs were produced in thin discs of the bone by enforcing the flow of ionic solution through the disc sample by means of a plunger driven at constant speed through a cylinder in an Instron testing machine, cf. Fig. 23. For all solutions and specimens tested the peak voltage Φ_s, produced as electrolyte, was forced through a given slab of the tissue and was proportional to the crosshead speed.

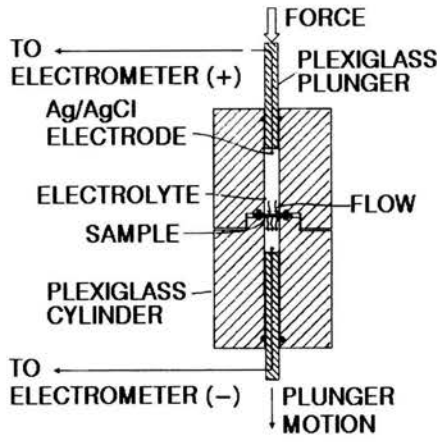

FIGURE 23. Streaming apparatus. The Instron crosshead forces the top plunger downward at a given speed as applied force and generated voltage are monitored simultaneously, after Gross and Williams [60].

Next, in 1988 Otter *et al.* [140] investigated the contributions made by the various constituents of bone in production of SPs; particularly, they proposed a method to determine which of the two main constituents of bone, the collagen or apatite plays greater role in the production of SPs. Following the approach due to Frank and Grodzinsky [47], selective removal of either main constituent - collagen or hydroxyapatite - of the tissue was performed by chemical means, and the SP was measured. Demineralized samples demonstrated the ZPs close to those of the whole bone samples, whereas anorganic samples had much smaller ZP. The collagen rather than the hydroxyapatite mineral is therefore involved as the constituent of whole bone dominating the SPs. This agrees with the observation that collageneous tissues containing no mineral phase, as tendon and cartilage, also exhibit SPs.

Weinbaum *et al.* [200] described in 2001 new mechanical models for the deformation of the actin filament bundles in kidney microvilli and osteocytic cell processes to see whether these cellular extensions, like the stereocilia on hair cells in the inner ear, can function as mechanotransducers when subject to physiological flow. In the case of bone cell processes it was shown that the actin filament bundles have the effective Young's modulus that is 200 times greater than that measured for the actin gel in the cell body. Moreover, the authors showed that the fluid drag forces on the pericellular matrix which tethers the cell processes to the canalicular wall can produce a 20-100 fold amplification of bone tissue strains in the actin filament bundle of the cell process.

10.2. Experiments on influence of SP on bone morphology

To get insight into the biological response of bone to mechanical loading at the cellular level the suggestion was made in 1990 that bone cells *in situ* are capable to respond to mechanical stimuli, cf. Nijwede and Burger [133], Cowin *et al.* [24]. These authors concluded that there are several possible processes by which the bone cell receives the strain signal. The direct mechanical deformation of the cell membrane may be sufficient to activate stretch sensitive membrane receptor sites, or the electrical charges produced by SPs act directly on the osteocytic cell membranes, possibly affecting the voltage dependent channels of those membranes. Other processes were reviewed by Moss [125]. For more details the reader is referred to the paper by Cowin in this volume, cf. also [97].

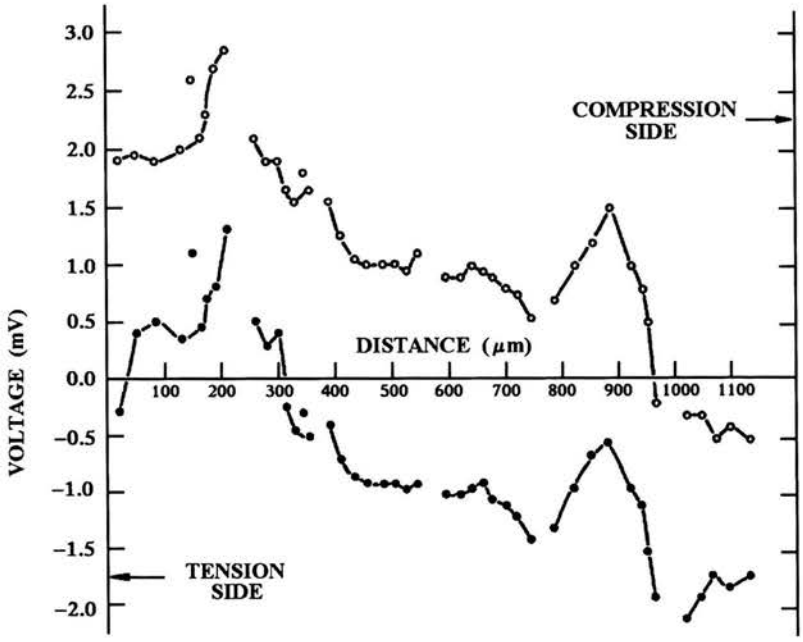

FIGURE 24. Microelectrode potential vs. distance accross transverse section of cortical bone in four-point bending. Open circles are values of potential measured relative to electrode on compression side of specimen and closed circles are potentials relative to tension side, after Starkebaum *et al.* [178].

The relationship between bone morphology and the SPs and, in particular, the spatial relationship between fluid flow pathways and bone cells permits to determine the magnitude of local electric fields appearing when fluid moves through the pores of bone. In a series of experiments performed

since 1979 and reported by Iannacone *et al.* [82], Starkebaum *et al.* [178], Pienkowski and Pollack [144], cf. also Pollack in Cowin [26, Chap. 24], microelectrodes were used to map the electrical potentials in wet bone during cyclic 1 Hz deformation. Specifically, machined bone specimens were loaded in four-point bending and the electrical potentials were measured with osteons to resolution of order $\pm 5\mu$m, see Fig. 24.

Possible influence of mechanical excitation on bone remodelling *via* the SPs was studied Beck *et al.* [9] in 2002. Under predominantly axial and bending loads, significantly different strain and strain gradients were generated at two recording sites of turkey bone during *in vivo* experiment, cf. Fig. 25.

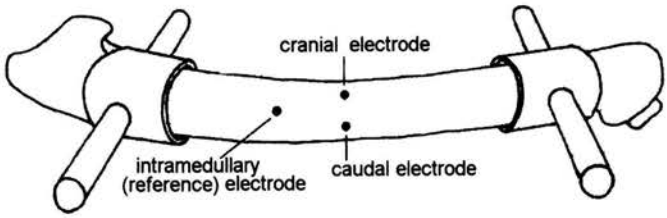

FIGURE 25. Turkey ulna preparation with electrode placement sites, after [9].

These authors observed previously unknown property of living bone: the sign of the ZP is different in different parts of the bone: it is negative at the caudal site and positive at the cranial site. This observation contradicts theoretical model of the SPs production *in vitro* in cylindrical (isotropic homogeneous poroelastic) samples in four-point bending which predicts that the SPs should be the smallest at the site of minimum strain and the largest at the site of maximum surface strain gradients within the matrix of the structure, cf. Spirt, Pollack [176]. Thus Beck's group finding appears to contradict an intuitive sense of how bone matrix driven fluid flow should be distributed in loaded bone. The reasons for such a departure are unclear.

10.3. Streaming potentials in bones under pressure variations

According to Rubin *et al.* [161] high frequency bone strains in the range 15-30 Hz might have significant influence on the morphological adaptation of bone tissue. Next, Turner *et al.* [193] examined the magnitude of high frequency strains during various activities. They measured strains in the forelimbs of dogs during walking, standing and with their limbs unweighted. As negative controls, the authors measured strains while the dogs were tranquilized and after sacrifice. Strains in the range 15-30 Hz were not significantly greater than controls for any activity except walking, in which they were less

than 4% as large as in the 0-15 Hz range. The high frequency strains observed during walking seemed to occur prior to footfall, suggesting that they were not the result of foot strike. The biological significance of high frequency bone strains has yet to be determined, but may be smaller than originally proposed because of the relatively low magnitude of these strains.

The question of determining the anatomical site that is the source of the experimentally observed strain generated potentials (SGPs) in bone tissue is not yet resolved. There are two candidates for the anatomical site that is the SGPs source: the collagen-hydroxyapatite porosity and the larger size lacunar-canalicular porosity. It was argued, on the basis of experimental data and the reasonable model, that the site of the SGPs in bone is the collagen-hydroxyapatite porosity. The theoretically predicted pore radius necessary for the SGPs to reside in this porosity is 16 nm, which is somewhat larger than the pore radii estimated by another method according to which the preponderance of the pores were estimated to be in the range 5–12.5 nm. However, this pore size is significantly larger than the 2 nm size of the small tracer, microperoxidase, which appears to be excluded from the mineralized matrix.

Cowin *et al.* [25] presented in 1995 a similar model, one in which the effects of fluid dynamic drag of the cell surface matrix in the bone canaliculi are included and showed that it is possible to generate of SGPs to be associated with the larger size lacunar-canalicular porosity when the hydraulic drag and electrokinetic contribution of the bone fluid passage through the cell coat (glycocalyx) is considered. The consistency of the SGP data with this model was demonstrated. The results obtained suggest that the current leakage is small for the *in vitro* studies in which the strain generated potentials have been measured.

According to Weinbaum *et al.* [199] the osteocytes, although not responsive to substantial fluid pressures, can be stimulated by relatively small fluid shear stresses acting on the membranes of their osteocytic processes. Biot's porous media theory was used to relate the combined axial and bending loads applied to a bone to the flow past the osteocytic processes in their canaliculi. In this theory, the bone pores of interest are the proteoglycan filled fluid annuli that surround the osteocytic processes in the canaliculi. These authors claim that previously predicted fluid pore pressure relaxation times were a hundred-fold too short for the lacunar-canalicular porosity because the fluid drag associated with proteoglycan matrix on the surface membrane of the osteocyte and its cell processes was neglected. Zeng *et al.* [211] developed in 1994 a theoretical model to predict the fluid shear stress and SP at the surface of osteocytic processes in the lacunar-canalicular porosity of an osteon when the osteon is subject to mechanical loads that are parallel or

perpendicular to its axis. The theory predicts that the pore pressure relaxation time, τ_d, for a 150-300 μm diameter osteon with the foregoing matrix structure of approximately the order of 0.03-0.13 sec, and that the amplitude of the mean fluid shear stress on the membrane of the osteocytic process at the mean areal radius of the osteon has a maximum at 28 Hz if τ_d=0.06 sec.

Klein-Nulend *et al.* [86], [87] used fluid flow for mechanical stimulation of the osteocytes to test the hypothesis, developed by Cowin and associates, that in intact bone the osteocytes are mechanically activated by flow of interstitial fluid through the lacuno-canalicular porosity, cf. Cowin *et al.* (1991), Weinbaum *et al.* (1994), Cowin *et al.* (1995), and the paper by Cowin [27], his paper in this volume and references therein. According to Murray and Rushton [128] and Neidlinger-Wilke *et al.* [129] the magnitude of strains *in vitro* required to obtain a cellular response, is on the order of 13%. Under physiological loads the strains on the order of 0.2% only are reported, cf. [26]. Hence the need for the search of mechanotransduction mechanisms, cf. the paper by Cowin in this volume.

Klein-Nulend *et al.* [87] studied in 1995 the response of isolated osteocytes derived from embryonic chicken calvariae to intermittent hydrostatic compression as well as pulsating fluid flow (PFF), and compared their response to that of osteoblasts and periosteal fibroblasts. These data provide evidence that osteocytes are the most mechanosensitive cells in bone involved in the transduction of mechanical stress into a biological response. The results obtained support the hypothesis that stress in bone causes fluid flow in the lacunar- canalicular system, which stimulates the osteocytes to produce factors that regulate bone metabolism.

Rubin *et al.* [163] studied in 1996 the effect of low frequency electric fields on osteoclast-like cell formation. The experiments demonstrate that extremely low intensity, low frequency sinusoidal electric fields suppress the formation of osteoclast-like cells in marrow culture. The *in vitro* results support *in vivo* findings that demonstrate that electric fields inhibit the onset of osteopenia and the progression of osteonecrosis; this suggests that extremely low frequency fields may inhibit osteoclast recruitment *in vivo*.

Zhang *et al.* [212] proposed in 1997 a cable model to estimate the spatial distribution of intracellular electric potential and current, from the cement line to the lumen of an osteon, as the frequency of the loading and the conductance of the gap junction are altered. The model predicts that the characteristic diffusion time for the spread of current along the membrane of the osteocytic processes is equal to 0.03 s. The cable behaves as a high-pass, low-pass filter cascade with a maximum in the spectral response for the intracellular potential at approximately 30 Hz. This behavior could be related to the experiments of Rubin and McLeod [162] who showed that

living bone appears to be selectively responsive to mechanical loading in a specific frequency range (15–30 Hz).

Rubin *et al.* [164] showed in 2001 that after mechanically stimulating the hindlimbs of adult sheep on a daily basis for a year with 20–minute bursts of very-low-magnitude, high-frequency vibration, the density of the trabecular bone in the proximal femur is significantly increased (by 34%) compared to controls. As the strain levels generated by this treatment are three orders of magnitude below those that damage bone tissue, this anabolic, non-invasive stimulus may have potential for treating skeletal conditions such as osteoporosis.

The luminal surface of endothelial cells is lined with the glycocalyx, a network structure of glycoproteins probably 50 to 100 nm thick. Squire *et al.* [177] suggested that a relatively regular fibre-matrix structure may be responsible for the ultrafiltration properties of microvascular walls, both when the endothelium is continuous and when it is fenestrated. Positive structural evidence demonstrating an underlying periodicity in the glycocalyx was difficult to obtain. These authors presented a structural analysis of glycocalyx samples prepared in a variety of ways for electron microscopy investigations. Using computed autocorrelation functions and Fourier transforms of representative areas of the electron micrograph images, they have shown that there is an underlying three-dimensional fibrous meshwork within the glycocalyx with characteristic spacings of about 20 nm.

Recently, Weinbaum *et al.* [201] provided an overview of the endothelial surface layer or glycocalyx in several roles: as a transport barrier, as a porous hydrodynamic interface in the motion of red and white cells in microvessels, and as a mechanotransducer of fluid shearing stresses to the actin cortical cytoskeleton of the endothelial cell. These authors examined those functions from a new perspective, the quasiperiodic ultrastructural model proposed by Squire *et al.* [177] for the 3D organization of the endothelial surface layer and its linkage to the submembranous scaffold. It was shown that the core proteins in the bush-like structures comprising the matrix have a flexural rigidity that is sufficiently stiff to serve as a molecular filter for plasma proteins and as an exquisitely designed transducer of fluid shearing stresses. However, the flexural rigidity is inadequate to prevent the buckling of these protein structures during the intermittent motion of red cells or the penetration of white cell microvilli. In these cellular interactions, the viscous draining resistance of the matrix is essential for preventing adhesive molecular interactions between proteins in the endothelial membrane and circulating cellular components.

11. Recent developments and final remarks

Liquid flows in capillary porous systems leading to the generation of SPs have attracted attention of biologists, mechanicists and physicists since the discovery of electrokinetic transport. Electrokinetics links the mechanical and electrical phenomena, and plays a role in transport of ionic species. While appearance of SPs in different biological processes is indisputable, its determination by measurement or calculation is achieved only in simplified conditions. Moreover, because of complexity of biological systems the role of SPs has not yet been completely clarified.

Cells subjected to fluid flow are exposed to two types of stimuli, fluid-induced drag forces (or fluid shear stress) and streaming electrical potentials. The convective current establishes an electrokinetic force created by the flow-dependent transport of mobile ions in the media over the charged cell surfaces. According to Beck *et al.* [9] bone cells respond to strains indirectly *via* electrokinetic phenomena although the self mechanism of interaction is obscure. The sensor for bone adaptation is widely believed to be the osteocyte, cells which are very sensitive to fluid shear stress. However, to date we have only a very preliminary knowledge of how these cells function in this respect, cf. You *et al.* [208].

Becker and his co-workers have explored tissue electrical properties in connection with growth, repair and regeneration, cf. [6], [10]- [14], see also [108]. Partial limb regeneration in rats was stimulated by application of weak electrical signals. Electrical signals in amphibians, which can naturally regenerate lost limbs, differ from those in mammals, which ordinarily do not regenerate lost limbs. Cartilage exhibits electrical response to applied force. Electrical properties of bone are relevant not only to a hypothesized feedback mechanism for bone remodelling, but also in to external electrical stimulation of bone to aid its healing and repair. Axial electric signals were considered in the light of the ability of salamanders to regenerate their limbs. Biological effects of electrical signals were used to stimulate the regrowth of portions of amputated limbs in rats which usually do not regenerate.

Chow and Chambers [22], looking for the mechanisms by which mechanical stimuli are translated into new bone, studied the role of prostaglandins (PGs). They found that PGs are essential for the transduction of mechanical stimuli into bone formation, and also that there may be two distinct phases of PGs dependency in the response of bone to mechanical loading: an early phase associated with the immediate loading period and a later phase associated with osteogenic interactions entrained by the early phase.

In a study on cell signalling after mechanical stimulation, monolayer cultures of osteocytes, isolated from embryonic chicken calvariae, responded to

pulsated fluid flow (PFF) with a sustained release of prostaglandins E_2 and I_2 (PGE_2 and PGI_2, respectively). Osteocytes were much more responsive than osteoblasts, and intermittent hydrostatic compression had less effect than fluid flow. *In vivo*, prostaglandins were found to be essential for the transduction of mechanical stimuli into bone formation, whereas *in vitro* as well as *in vivo* prostaglandins stimulate osteoblastic cell proliferation and bone formation, cf. Ajubi *et al.* [1]. Fluid flow rapidly increased intracellular calcium in bone cells, an effect that was inhibited using neomycin or gadolinium, suggesting calcium influx *via* stretch-activated channels as well as release from intracellular stores. These studies confirmed the efficacy of fluid flow as a mechanical stimulus for bone cells, which was also concluded from *in vivo* studies.

The importance of nitric oxide (NO) and prostaglandins as mediators of loading-induced adaptive bone response has been substantiated in a number of studies. Transient rapid increase of NO release was found in several *in vitro* systems, including osteocyte monolayer cultures and bone organ cultures. *In vivo*, the NO inhibitor L-NAME suppressed mechanically induced bone formation in rats. Turner *et al.* [194] hypothesized that NO may act as an intermediary in the transduction of mechanical loading of bone into a bone formation response. In the study, 48 rats were divided into the three treatment groups: control, treated with N omega-nitro-L-arginine methyl ester (L-NAME; an inhibitor of nitric oxide synthase), and treatment with D-NAME (the less active enantiomer of L-NAME). Treatment with L-NAME reduced the rate of mechanically induced bone formation by 66% compared with the control group. Bone formation rates in nonloaded or sham-loaded limbs were not affected by L-NAME treatment. The results suggested that nitric oxide may play a role in the transduction of a mechanical stimulus into a biological response in bone.

Forwood [46] has used *in vivo* indomethacin blockade of bone formation to illustrate the role of prostaglandins. Prostaglandins are a member of the lipid class of biochemicals and are known for their potent physiological properties. Prostaglandins act in a manner similar to that of hormones, by stimulating target cells into action. However, they differ from hormones in that they act locally, near their site of synthesis, and they are metabolized very rapidly. Another unusual feature is that the same prostaglandins act differently in different tissues. Klein-Nulend *et al.* [88] examined the effects of 1 h pulsating fluid flow on three types of prostaglandin production. One hour after PFF removal, the production of prostaglandins was still enhanced. These results suggested that prostaglandins can be early mediators of the response of bone cells to mechanical stress. Thus, prostaglandins are an important part of the mechanobiochemical signaling.

In the same year 1997 Salter *et al.* [165] indicated that bone cells respond to mechanical stimuli, but the transduction mechanisms responsible are not fully understood. Integrins, a family of heterodimeric transmembrane glycoproteins, which link components of the extracellular matrix with the actin cytoskeleton, have been implicated as mechanoreceptors. The role of integrins in the transduction of cyclic mechanical stimuli to human bone cells (HBC) results in changes in membrane potential. HBC showed membrane depolarization following 0.104 Hz mechanical stimulation and membrane hyperpolarization following stimulation at 0.33 Hz. Differential electrophysiological response of HBC to different frequencies of mechanical strain suggests that integrins act as HBC mechanoreceptors with distinct signalling pathways being activated by different frequencies of mechanical stimuli.

Hung et al. [78] have investigated the role of mitogen-activated protein kineses (MAPKs) in chondrocyte mechanotransduction. The authors' hypothesis was that MAPKs participate in fluid flow-induced chondrocyte mechanotransduction. To test their hypothesis the authors studied cultured chondrocytes subjected to a well-defined mechanical stimulus generated with a laminar flow chamber. The extracellular signal-regulated kinases 1 and 2 (ERK 1/2) were activated 1.6-3-fold after 5-15 min of fluid flow exposure corresponding to a chamber wall shear stress of 1.6 Pa. To assess downstream effects of the activated MAPKs on transcription, flow studies were performed using chondrocytes transfected with a chimeric luciferase construct containing 2.4 kb of the promoter region along with exon 1 of the human aggrecan gene. Two-hour exposure of transfected chondrocytes to fluid flow significantly decreased aggrecan promoter activity by 40%. This response was blocked by treatment of chondrocytes with the MEK-1 inhibitor PD98059. These findings demonstrate that, under the conditions of the study, fluid flow-induced signals activate the MEK-1/ERK signalling pathway in articular chondrocytes, leading to down regulation of expression of the aggrecan gene.

Cytosol is the fluid in which the organelles of the cytoplasm are suspended - it is also known as the ground substance of the cell. Cytosolic calcium modulates the activity of osteoclasts, large multinucleate cells that resorb bone, [142]. Miyauchi *et al.* [120] studied already in 1990 the mechanisms of Ca^{2+} entry and their effects on cell function in cultured chicken osteoclasts and putative osteoclasts produced by fusion of mononuclear cell precursors. The ions K^+ produced dose-dependent increases of cytosolic calcium $[Ca^{2+}]_i$ in osteoclasts on glass coverslips. Increasing extracellular Ca^{2+} $[Ca^{2+}]_e$ induced Ca^{2+} release from intracellular stores and Ca^{2+} influx. The effects of $[Ca^{2+}]_e$ on $[Ca^{2+}]_i$ suggests the presence of a Ca^{2+} receptor on the osteoclast cell membrane that could be coupled to mechanisms regulating cell function.

Expression of the $[Ca^{2+}]_e$ effect on $[Ca^{2+}]_i$ was similar in the presence or absence of bone matrix substrate. We recall that the indices e and i are used to denote extracellular and intracellular ions respectively.

In 2000 Miyauchi *et al.* [121] documented for the first time a volume-sensitive Ca^{2+} influx pathway in osteocytes, which transmits loading-induced signals into bone formation. Stretch loading by swelling rat and chicken osteocytes in hypo-osmotic solution induced a rapid and progressive increase of cytosolic calcium concentration, $[Ca^{2+}]_i$. The influx of extracellular Ca^{2+} explains the increased $[Ca^{2+}]_i$ that paralleled the increase in the mean cell volume.

Recently, to assess the involvement of vascular endothelial growth factor (VEGF) in the pathology of osteoarthritic (OA) cartilage, Enomoto *et al.* [39] examined the expression of VEGF isoforms and their receptors in the cartilage, and the effects of VEGF on the production of matrix metalloproteinases (MMPs) and tissue inhibitors of metalloproteinases (TIMPs) in OA chondrocytes. Their results suggest the possibility that VEGF is implicated for the destruction of OA cartilage through the increased production of MMPs.

The cytoskeloton is physically linked to many cellular components, and some of them may be involved in the flow induced production of prostaglandins (PGs). To maintain its structural competence, the skeleton adapts to changes in its mechanical environment. Osteocytes are generally considered the bone mechanosensory cells that translate mechanical signals into biochemical, bone metabolism-regulating stimuli necessary for the adaptive process.

Prostaglandin E_2 (PGE_2) is an endogenous hormone of adrenal zona glomerulosa cells and is released in response to stimulation by agonists such as angiotensin. It stimulates the release of aldosterone from cultured bovine adrenal zona glomerulosa cells, cf. Csukas *et al.* [28]. The signal transduction pathways in osteocytes through which mechanical stress generates an acute release of prostaglandin E_2 (PGE_2) were investigated by Ajubi *et al.*[2].

Isolated chicken osteocytes were subjected to 10 min of pulsating fluid flow (PFF; 0.7 ± 0.03 Pa at 5 Hz), and PGE_2 release was measured. Blockers of Ca^{2+} entry into the cell or Ca^{2+} release from internal stores markedly inhibited the PFF-induced PGE_2 release, as did disruption of the actin cytoskeleton by cytochalasin B. Specific inhibitors of Ca^{2+} - activated phospholipase C, protein kinase C, and phospholipase A_2 also decreased PFF-induced PGE_2 release. These results are consistent with the hypothesis that PFF raises intracellular Ca^{2+} by an enhanced entry through mechanosensitive ion channels in combination with Ca^{2+} - and inositol trisphosphate (the product of phospholipase C)-induced Ca^{2+} release from intracellular stores. Ca^{2+} and protein kinase C then stimulate phospholipase A_2 activity, arachidonic

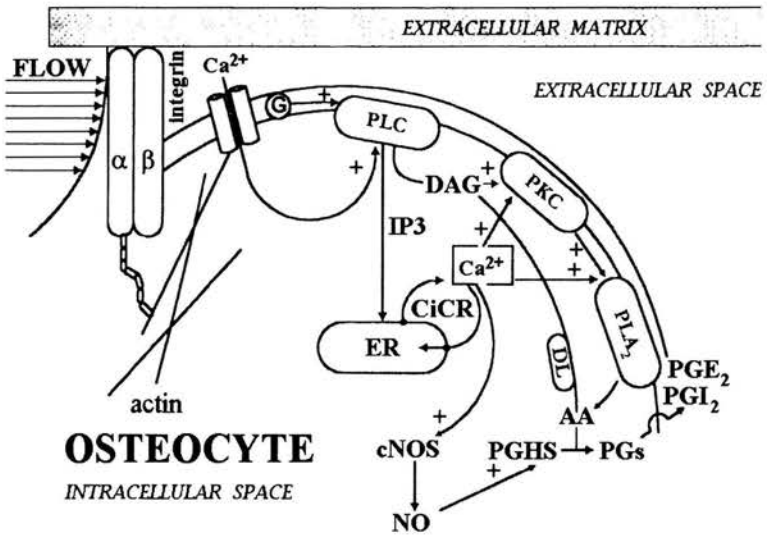

FIGURE 26. Schematic representation of possible signal transduction routes involved in the mechanical activation of osteocytes. Notation: PLA_2 - cytosolic phospholipase A_2, PLC - phospholipase C, ER - endoplasmic reticulum, DAG - diacylglycerol, DL - diacylglycerollipase, PKC - protein kinase C, IP_3 - inositol trisphosphate, CiCR - calcium induced calcium release, cNOS - constitutive nitric oxide synthase, NO - nitric oxide, PGHS - prostaglandin H synthase, AA - arachidonic acid, PGs - prostaglandins, PGE_2 and PGI_2 - prostaglandin E_2 and I_2, + denotes activation. G protein transduces intracellular signalling pathways. Fluid shear stresses result from the load induced fluid flow (parallel arrows), after Ajubi *et al.* [2].

acid production, and ultimately PGE_2 release. Figure 26 shows a scheme of possible signal transduction routes involved in the mechanical activation of osteocytes. The osteocyte is attached *via* integrins to the surrounding extracellular matrix. Fluid shear stresses activate cellular components either directly by membrane perturbation or through force transmission *via* integrin - cytoskeletal structures, leading to enhanced prostaglandin synthesis.

Bone formation is enhanced by mechanical loading, but the response to mechanical loading is variable, with some individuals exhibiting robust osteogenic responses while others respond modestly. Thus, mechanosensitivity — the ability of bone tissue to detect mechanical loads — could be under genetic control. Robling and Turner [157] applied controlled mechanical loading to the ulnae of 20-week-old (adult) female mice derived from three different inbred strains (C3H/He, C57BL/6, and DBA/2), and measured the bone formation response with fluorochrome labels. Mechanical properties, including the mechanical strain, second moments of area, and material properties of

cortical bone, were measured in a group of calibration animals not subjected to in vivo loading. The C3H/He mice were significantly less responsive to mechanical loading than the other two biological strains. Material properties (flexural elastic modulus, ultimate stress) were the greatest in the C3H/He cortical tissue. Based on the presumed role of osteocytes in strain detection, the osteocyte lacuna population densities in decalcified midshaft ulna sections were measured. The osteocyte lacuna density was not related to mechanosensitivity. These observations suggest a significant role of genetic factor for bone mechanosensitivity, apart from electrical and mechanical phenomena.

Acknowledgement

The authors were partially supported by the EC project MIAB, contract QLK6-CT-1999-02024. The first author appreciates also the support by the Ministry of Science and Information Technology through the grant No 4 T11F 003 25.

References

1. N.E. AJUBI, J. KLEIN-NULEND, P.J. NIJWEIDE , T. VRIJHEID-LAMMERS, M.J. ALBLAS AND E.H. BURGER, Pulsating fluid flow increases prostaglandin production by cultured chicken osteocytes–a cytoskeleton-dependent process, *Biochem. Biophys. Res. Commun.*, Vol.225(1), pp.62-8, 1996.

2. N.E. AJUBI, J. KLEIN-NULEND, M.J. ALBLAS, E.H. BURGER AND P.J. NIJWEIDE, Signal transduction pathways involved in fluid flow-induced PGE_2 production by cultured osteocytes, *American Journal of Physiology*, Vol.276(1 Pt 1), pp.E171-8, 1999.

3. J.C. ANDERSON and C. ERIKSSON, Electrical properties of wet collagen, *Nature*, Vol.218, pp.166-68, 1968.

4. C.G. ARMSTRONG, W.M. LAI, V.C. MOW, An analysis of the unconfined compression of articular cartilage, *Journal of Biomechanical Engineering*, Vol.106(2), pp.165-73, 1984.

5. G.A. ATESHIAN , M.A. SOLTZ , R.L. MAUCK, I.M. BASALO, C.T. HUNG and W.M. LAI, The role of osmotic pressure and tension-compression nonlinearity in the frictional response of articular cartilage, *Transport in Porous Media*, Vol.50(1/2), pp.5-33, 2003.

6. C.A.L. BASSETT and R.O. BECKER, Generation of electric potentials by bone in response to mechanical stress, *Science*, Vol.137, pp.1063-64, 1962.

7. C.A.L. BASSETT, R.J. PAWLUK and R.O. BECKER, Effects of electric currents on bone *in vivo*, *Nature*, Vol.204, pp.652-54, 1964.

8. L. BEADLING Yasuda electrified fracture healing (This pioneer of electrical stimulation was a gifted investigator as well as Oriental scholar and poet), http://www.geocities.com/beadling/Yasuda.html.

9. B.R. BECK, Y.-X. QIN, K.J. MCLEOD and M.W. OTTER, On the relationship between streaming potential and strain in an *in vivo* bone preparation, *Calcif. Tissue Int.*, Vol.71, pp.335-43, 2002.

10. R.O. BECKER, Search for evidence of axial current flow in peripheral nerves of salamander, *Science*, Vol.134, pp.101-102 (1961a).

11. R.O. BECKER, The bioelectric factors in amphibian limb regeneration, *J. Bone Joint Surg.*, Vol.43-A, pp.643-56 (1961b).

12. R.O. BECKER, C.A.L. BASSETT and C.H. BACHMAN, Bioelectrical factors controlling bone structure, *Bone Biodynamics*, ed. H.M. Frost, pp.209-232, Little Brown, Boston 1964.

13. R.O. BECKER, Electrical behavior of cartilage during loading, *Science*, Vol.178, pp.982-83 (1972a).

14. R.O. BECKER, Stimulation of partial limb regeneration in rats, *Nature*, Vol.235, pp.109-111 (1972b).

15. R.O. BECKER, The significance of bioelectric potentials, *Bioelectrochemistry and Bioenergetics*, Vol.1, pp.187-199, 1974.

16. L.J. BONASSAR, J.L. STINN, C.G. PAGUIO, E.H. FRANK, V.L. MOORE, M.W. LARK, J.D. SANDY, A.P. HOLLANDER, A.R. POOLE and A.J. GRODZINSKY , Activation and inhibition of endogenous matrix metalloproteinases in articular cartilage: Effects on composition and biophysical properties, *Archives of Biochemistry and Biophysics*, Vol.333(2), pp.359-67, 1996.

17. E.M. BRADBURY, R.E. BURGE, J.T. RANDALL and G.R. WILKINSON, The polypeptide chain configurations of native and denaturated collagen fibres, *Disc. Faraday Soc.*, No.25: Configurations and interactions of macromolecules and liquid crystals, pp.173-85, 1958.

18. E.H. BURGER and J. KLEIN-NULEND, Mechanotransduction in bone — role of the lacuno-canalicular network, *The FASEB Journal*, Vol.13, pp.S101-S112, 1999.

19. M.D. BUSCHMANN, A.J. GRODZINSKY, A molecular model of proteoglycan-associated electrostatic forces in cartilage mechanics, *J. Biomech. Eng.*, Vol.117(2), pp.179-92, 1995.

20. D.L. CHAPMAN, A contribution to the theory of electrocapillarity, *Phil Mag.*, Vol.25, pp. 475-81, 1913.

21. S.S. CHEN, Y.H. FALCOVITZ, R. SCHNEIDERMAN, A. MAROUDAS and R.L. SAH, Depth-dependent compressive properties of normal aged human femoral head articular cartilage: relationship to fixed charge density, *Osteoarthritis & C*artilage, Vol.9(6), 561-9, 2001.

22. J.W. CHOW and T.J. CHAMBERS, Indomethacin has distinct early and late actions on bone formation induced by mechanical stimulation, *American J. Physiol.*, Vol.267(2) Pt 1, pp.E287-92, 1994.

23. B. COHEN, W.M. LAI, V.C. MOW, A transversely isotropic biphasic model for unconfined compression of growth plate and chondroepiphysis, *Journal of Biomechanical Engineering* , Vol.120(4), pp.491-6, 1998.

24. S.C. COWIN, L. MOSS-SALENTIJN and M.L. MOSS, Candidates for the mechanosensory system in bone, *J. Biomech. Eng.*, Vol.113, pp.191-197, 1991.

25. S.C. COWIN, S. WEINBAUM and YU ZENG, A case for bone canaliculi as the anatomical site of strain generated potentials, *J. Biomech.*, Vol.28, pp.1281-97, 1995.

26. S.C. COWIN, editor, *Bone Mechanics Handbook*, CRC Press, Boca Raton-London-New York-Washington D.C., 2001.

27. S.C. COWIN, Adaptive elasticity: a review and critique of a bone tissue adaptation model *Engineering Transactions Rozprawy Inżynierskie*, Vol. 51(2-3), pp.113-93, 2003.

28. S. CSUKAS, C.J. HANKE, D. REWOLINSKI, W.B. CAMPBELL, Prostaglandin E_2-induced aldosterone release is mediated by an EP_2 receptor, *Hypertension*, Vol. 31(2), pp.575-81, 1998.

29. A. CURNIER, A., QI-CHANG HE and P. ZYSSET, Conewise linear elastic materials, *J. Elasticity*, Vol.37(1), pp.1-38, 1994-1995.

30. P. DEBYE and E. HÜCKEL, Zur Theorie der Elektrolyte, *Phys. Zft*, Vol.24, pp. 185-206, Zur Theorie der Elektrolyte.II., *Phys. Zft*, Vol. 24, pp.305-25, 1923.

31. P. DEBYE, Osmotische Zustandsgleichung und Aktivität verdünnter starker Elektrolyte, *Physik. Zeitschr.*, Vol.25, pp.97-107, 1924.

32. P. DEBYE UND E. HÜCKEL, Bemerkungen zu einem Satze über die kataphoretische Wanderunggeschwindigkeit suspendierter Teilchen, *Phys. Zft*, Vol.25, pp.49-52, 1924.

33. B.V. DERJAGUIN and L.D. LANDAU, Theory of the stability of strongly charged lyophobic sols and of the adhesion od strongly charged particles in solutions of electrolytes, *Acta Physicochim. URSS*, Vol.14, pp.733-62, 1941.

34. P. DUTTA and A. BESKOK, Analytical solution of combined electroosmotic/pressure driven flows in two-dimensional straight channels: finite Debye layer effects, *Anal. Chem.*, Vol.73, pp.1979-86, 2001.

35. P. DUTTA, M.J. KIM, K.D. KIHM and A. BESKOK, Electroosmotic flow in a grooved micro-channel configuration: a comparative study of μ-PIV measurements and numerical simulations, *Micro-Electro-Mechanical Systems. 2000 ASME International Mechanical Engineering Congress and Exposition*, 11-16 Nov. 2001, New York 2001.

36. M. EDLICH, C.E. YELLOWLEY, C.R. JACOBS, H.J. DONAHUE , Oscillating fluid flow regulates cytosolic calcium concentration in bovine articular chondrocytes, *Journal of Biomechanics*, Vol. 34(1), pp.59-65, 2001.

37. B.T. EDMONDS, J. MURRAY and J. CONDEELIS, pH regulation of the F-actin binding properties of Dictyostelium elongation factor, *J. Cell. Biol.*, Vol.270, pp. 15222-230, 1995.

38. M. ELIMELECH, J. GREGORY, X. JIA and R.A. WILLIAMS, *Particle deposition and aggregation: measurement, modeling and simulation*, Butterworth-Heineman, Oxford-London-Boston, 1995.

39. H. ENOMOTO, I. INOKI, K. KOMIYA, T. SHIOMI, E. IKEDA, K.-I. OBATA, H. MATSUMOTO, Y. TOYAMA and Y. YASUNORI OKADA, Vascular endothelial growth factor isoforms and their receptors are expressed in human osteoarthritic cartilage, *American J. Pathol.*, Vol.162, pp.171-81, 2003.

40. N.G. ESIPOVA, N.S. ANDREEVA and T.V. GATOVSKAYA, On the role of water in the collagen structure, [in Russian], *Biofizika*, Vol.3, pp.529-40, 1958.

41. H. FELLE, pH as a second messenger in plants, in: BOSS, W.F., MORRÉ, D.J., *Second Messengers in Plant Growth and Development*, pp.145-66, Alan R. Liss, New York 1989.

42. H.H. FELLE, E. KONDOROSI, A. KONDOROSI, M. SCHULTZE, Rapid alkalinization in alfalfa root hairs in response to rhizobial lipochitooligosaccharide signals, *Plant J.*, Vol.10, pp.295-301, 1996.

43. L. G. FEOKTISTOV, Kapillarnyy elektrometr, in: *'Fizicheskiy Entsiklopedicheskiy Slovar'*, Vol. 2, pp. 278, Izd. "Sovetskaya Entsiklopediya", Moskva, 1962.

44. L. G. FEOKTISTOV, Elektrokapillarnye yavleniya, in: *'Fizicheskiy Entsiklopedicheskiy Slovar'*, Vol. 5, pp.457-8, Izd. "Sov. Entsikl.", Moskva 1966.

45. M. FILEK, M. ZEMBALA and M. SZECHYŃSKA-HEBDA, The influence of phytohormones on zeta potential and electrokinetic charges of winter wheat cells, *Z. Naturforsch.*, Vol.57c, pp.696-704, 2002.

46. M.R. FORWOOD, Inducible cyclo-oxygenase (COX-2) mediates the induction of bone formation by mechanical loading in vivo, *J. Bone Miner. Res.*, Vol.11(11), pp.1688-93, 1996.

47. E.H. FRANK and A.J. GRODZINSKY, Streaming potential detection of cartilage degeneration kinetics in vitro, *Trans. Bioelec. Repair Growth Soc.*, Vol.3, pp.16, 1983.

48. E.H. FRANK and A.J. GRODZINSKY, Cartilage electromechanics - I. Electrokinetic transduction and the effects of electrolyte pH and ionic strength, *J. Biomech.*, Vol.20, pp.615-27, 1987.

49. E.H. FRANK and A.J. GRODZINSKY, Cartilage electromechanics - II. A continuum model of cartilage electrokinetics and correlation with experiments, *J. Biomech.*, Vol.20, pp.629-39, 1987.

50. E.H. FRANK, A.J. GRODZINSKY, T.J. KOOB and D.R. EYRE, Streaming potentials: a sensitive index of enzymatic degradation in articular cartilage, *J. Orthop. Res.*, Vol.5(4), pp.497-508, 1987.

51. E. FUKADA and YASUDA, On the piezoelectric effect of bone, *J. Phys. Soc. Japan*, Vol.12, pp.1158-62, 1957.

52. A. GALKA, J.J. TELEGA and R. WOJNAR, Modelling electric and elastic properties of cartilage, *Engineering Transactions*, Vol.49(2-3), pp.283-313, 2001.

53. M. GARON, A. LÉGARÉ, R. GUARDO, P. SAVARD and M.D. BUSCHMANN, Streaming potentials maps are spatially resolved indicators of amplitude, frequency and ionic strength dependent responses of articular cartilage to load, *J. Biomech.*, Vol.35, pp.207-16, 2002.

54. J.C. GHOSH, The abnormality of strong electrolytes, *Trans. Chem. Soc.*, Vol.113, pp.(449, 627, 707), 1918.

55. A.YA. GOKHSHTEIN, Electrolysis and surface phenomena. To the bicentenary of Volta's publication on the first direct-current source, [in Russian], *Usp. Fiz. Nauk*, Vol.170, pp.779-804, 2000.

56. G. GOUY, Sur la consitition de la charge électrique à la surface d'un électrolyte, C.R.A.S. Paris, Vol.149, pp.654-7, 1909.

57. S. GRABSKI, X.G. XIE, J.F. HOLLAND and M. SCHINDLER, Lipids trigger changes in the elasticity of the cytoskeleton in plant cells: a cell optical displacement assay for live cell measurements, *J. Cell Biol.*, Vol.126, pp.713-726, 1994.

58. D.C. GRAHAME, The electrical double layer and the theory of electrocapillarity, *Chem. Rev.*, Vol.41, pp.441-501, 1947.

59. I.S. GROMEKA, K teorii dvizheniya zhidkosti v uzkikh tsilindricheskikh trubkakh, 1882, cf.: *Sobraniye sochineniy*, Izd. AN SSSR, pp.149-71, 1952.

60. D. GROSS and W.S. WILLIAMS, Streaming potential and the electromechanical response of physiologically moist bone, *J. Biomech.*, Vol.15, pp.277-95, 1982.

61. R.M. GRYNKIEWICZ, M. POENIE and R.Y. TSIEN, Flow-induced calcium transients in single endothelial cells: spatial and temporal analysis, *J. Biol. Chem.*, Vol.280(6), pp.3440-50, 1985.

62. W.Y. GU, W.M. LAI and V.C. MOW, Transport of fluid and ions through a porous-permeable charged-hydrated tissue, and streaming potential data on normal bovine articular cartilage, *J. Biomech.*, Vol.26(6), pp.709-23, 1993.

63. W.Y. GU, W.M. LAI and V.C. MOW, A mixture theory for charged-hydrated soft tissues containing multi-electrolytes: passive transport and swelling behaviors, *J. Biomech. Eng.*, Vol.120(2), pp.169-180, 1998.

64. W.Y. GU, X.G. MAO, B.A. RAWLINS, J.C. IATRIDIS, R.J. FOSTER, D.N. SUN, M. WEIDENBAUM and V.C. MOW, Streaming potential of human lumbar anulus fibrosus is anisotropic and affected by disc degeneration, *J. Biomech.*, Vol.32(11), pp.1177-82, 1999.

65. J. GUERN, Y. MATHIEU, S. THOMINE, J.P. JOUANNEAU and J.C. BELOEIL Plant cells counteract cytoplasmic pH changes but likely use these pH changes as secondary messages in signal perception, *Curr. Top. Plant Biochem. Physiol.*, Vol.11, pp.249-269, 1992.

66. F. GUILAK, B.C. MEYER, A. RATCLIFFE and V.C. MOW, The effects of matrix compression on proteoglycan metabolism in articular cartilage explants, *Osteoarthritis & C*artilage, Vol.2(2), pp.91-101, 1994.

67. F. GUILAK, R.A. ZELL, G.R. ERICKSON, D.A. GRANDE, C.T RUBIN, K.J. MCLEOD and H.J. DONAHUE, Mechanically induced calcium waves in articular chondrocytes are inhibited by gadolinium and amiloride, *J. Orthopaedic Res.*, Vol.17(3), pp.421-9, 1999.

68. N. GÜZELSU and H. DEMIRAY, Recent advances Electromechanical properties and related models of bone tissues, *Int. J. Engng Sci.*, Vol.17, pp.813-851, 1979).

69. W.F. HARRINGTON and P.H. VON HIPPEL, The structure of collagen and gelatin, *Advances in Protein Chemistry*, Vol.16, pp.1-138, 1961.

70. D. HEINEGARD, A. OLDBERG, Structure and biology of cartilage and bone matrix noncollagenous macromolecules, *FASEB Journal*, Vol. 3(9), pp.2042-51, 1989.

71. H. HELMHOLTZ, Studien über electrische Grenzschichten, *Annalen der Physik und Chemie*, Neue Folge, VII (hgb. G. Wiedemann), Leipzig, pp.337-82, 1879.

72. D.C. HENRY, The cataphoresis of suspended particles. Part I.- The equation of cataphoresis, *Proc. R. Soc. London*, Vol.133A, pp.106-29, 1931.

73. B. HILLE, *Ionic Channels of Excitable Membranes*, Ed. 2, Sinauer Associates, Sunderland MA, 1992.

74. A.L. HODGKIN and A.F. HUXLEY, A quantitative description of ion currents and its applications to conduction and excitation in nerve membranes, *J. Physiol.* (Lond.), Vol.117, pp.500-44, 1952.

75. E. HÜCKEL, Die Kataphorese der Kugel, *Physik. Zeitschr.*, Vol.25, pp.204-10, 1924.

76. C.T. HUNG, F.D. ALLEN, S.R. POLLACK and C.T. BRIGHTON, What is the role of the convective current density in the real-time calcium response of cultured bone cells to fluid flow?, *J. Biomech.*, Vol.29, pp.1403-409, 1996a.

77. C.T. HUNG, F.D. ALLEN, S.R. POLLACK and C.T. BRIGHTON, Intracellural Ca^{2+} stores and extracellular Ca^{2+} are required in the real-time Ca^{2+} response of bone cells experiencing fluid flow, *J. Biomech.*, Vol.29, pp.1411-17, 1996b.

78. C.T. HUNG, D.R. HENSHAW, C.C.-B. WANG, R.L. MAUCK, F. RAIA, G. PALMER, PEN-HSIU GRACE CHAO, V.C. MOW, A. RATCLIFFE and W.B. VALHMU, Mitogen-activated protein kinase signaling in bovine articular chondrocytes in response to fluid flow does not require calcium mobilization, *J. Biomech.*, Vol.33(1), 73-80, 2000.

79. R.J. HUNTER, *Zeta Potential in Colloid Science - Principles and Applications*, Academic Press, London - New York - Orlando, 1981.

80. J.M.R.J. HUYGHE and J.D. JANSSEN, Quadriphasic mechanics of swelling incompressible porous media, *Int. J. Engng Sci.*, Vol.35, pp.793-802, 1997.

81. J.M. HUYGHE, Intra-extrafibrillar mixture formulation of soft charged hydrated tissues, *J. Theor. Appl. Mech.*, Vol.37, pp.519-36, 1999.

82. IANNACONE W., E. KOROSTOFF and S.R. POLLACK, Microelectrode studies of stress generated potentials obtained from uniform and non-uniform compression of human bone, *J. Biomed. Mat. Res.*, Vol.13(5), pp.753-63, 1979.

83. M. JIN and A.J. GRODZINSKY, Effect of electrostatic interactions of proteoglycans on the shear stiffness of cartilage: Molecular model of proteoglycans, *Macromolecules*, Vol.34, pp.8330-39, 2001.

84. Y.J. KIM, L.J. BONASSAR, A.J. GRODZINSKY, The role of cartilage streaming potential, fluid flow and pressure in the stimulation of chondrocyte biosynthesis during dynamic compression, *Journal of Biomechanics*, Vol.28(9), pp.1055-66, 1995.

85. TH.B. KINRAIDE, U. YERMIYAHU and G. RYTWO, Computation of surface electrical potentials of plant cell membranes - correspondence to published zeta potentials from diverse plant sources, *Plant Physiol.*, Vol.118, pp.505-12, 1998.

86. J. KLEIN-NULEND, A. VAN DER PLAS, C.M. SEMEINS, N.E. AJUBI, J.A. FRANGOS, P.J. NIJWEIDE and E.H. BURGER, Sensitivity of osteocytes to biomechanical stress in vitro, *The FASEB Journal*, Vol.9, pp.441-45, 1995.

87. J. KLEIN-NULEND, C.M. SEMEINS, N.E. AJUBI, P.J. NIJWEIDE and E.H. BURGER, Pulsating fluid flow increases nitric oxide (NO) synthesis by osteocytes but not periosteal fibroblasts–correlation with prostaglandin upregulation, *Biochem. Biophys. Res. Commun.*, Vol.217(2), pp.640-8, 1995.

88. J. KLEIN-NULEND, E.H. BURGER, C.M. SEMEINS, R.L. GAISZ and C.C. PILBEAM, Pulsating fluid flow stimulates prostaglandin release and inducible prostaglandin G/H synthase mRNA expression in primary mouse bone cells, *J. Bone Miner. Res.*, Vol.12(1), pp.45-51, 1997.

89. M.L. KNOTHE TATE, U. KNOTHE and P. NIEDERER, Experimental elucidation of mechanical load-induced fluid flow and its potential role in bone metabolism and functional adaptation, *Am. J. Med.Sci.*, Vol.316(3), 189-95, 1998a.

90. M. L. KNOTHE TATE, P. NIEDERER and U. KNOTHE, In vivo tracer transport through the lacunocanalicular system of rat bone in an environment devoid of mechanical loading, *Bone*, Vol.22, pp.107-117, 1998b.

91. M. L. KNOTHE TATE, "Whither flows the fluid in bone?" An osteocyte's perspective, *J. Biomech.*, Vol.36(10), pp.1409-24, 2003.

92. W.M. LAI, J.S. HOU and V.C. MOW, A triphasic theory for the swelling and deformation behaviors of articular cartilage, *J. Biomech. Eng.*, Vol.113(3), pp.245-58, 1991.

93. W.M. LAI, G.A. ATESHIAN, D.D. SUN and V.C. MOW, The electrical environment of chondrocytes in normal and OA cartilage: streaming potential vs. Nernst potential, *Biomechanics Symposium Honoring Dr. Fung's 80th Birthday*, BIO'99, Big Sky, Montana, June 16-20, 1999.

94. L.M. LAI, D.D. SUN, G.A. ATESHIAN, X.E. GUO and V.C. MOW, Effects of inhomogeneous fixed charges density on the electrical signal for chondrocytes in cartilage, in: *Mechanics in Biology*, AMD - vol. 242/BED - vol. 46, ed. by J. Casby, G. Bao, ASME, New York, pp. 201-213, 2000.

95. W.M. LAI, V.C. MOW, D.D. SUN and G.A. ATESHIAN, On the electric potentials inside a charged soft hydrated biological tissue: streaming potential versus diffusion potential, *J. Biomech. Eng.*, Vol.122(4), 336-46, 2000.

96. K. LAHIJI, A. POLOTSKY, D.S. HUNGERFORD and C. G. FRONDOZA, Cyclic strain stimulates proliferative capacity, α_2 integrin by human articular chondrocytes from osteoarthritic knee joints, *The University of Pennsylvania Orthopaedic Journal (UPOJ)*, Vol.15, pp.75-81, 2002.

97. T. LEKSZYCKI and J.J. TELEGA, Progress in functional adaptation of tissues and remodelling. Part II. Modelling and numerical methods, *Eng. Trans.*, 2004, submitted.

98. D.G. LEVITT, S.R. ELIAS and J.M. HAUTMAN, Number of water molecules coupled to the transport of sodium, potassium and hydrogen ions via gramicidin, nonactin and valinomycin, *Biochem. Biophys. Acta*, Vol.512, pp.436-51, 1978.

99. D.G. LEVITT, Streaming potential: Continuum expression applicable to very small nonuniform channels, *J. Chem. Phys.*, Vol.92, pp.6953-57, 1990.

100. D.G. LEVITT, Modeling of channels, *J. General Physiol.*, Vol.113, pp.789-94, 1999.

101. D.G. LEVITT, The use of streaming potential measurements to characterize biological ion channels, in: *Membrane Transport and Renal Physiology*, editors H.E. Layton, A.J.M. Weinstein, pp. 53-63, Springer, New York-Berlin, 2002.

102. L.P. LI, J. SOULHAT, M.D. BUSCHMANN and A. SHIRAZI-ADL, Nonlinear analysis of cartilage in unconfined ramp compression using a fibril reinforced poroelastic model, *Clinical Biomechanics* , Vol.14(9), pp.673-82, 1999.

103. E. M. LIFSHITS and L.D. PITAYEVSKIY, *Fizicheskaya kinetika* (*Physical Kinetics*), in Russian, "Nauka", Moskva, 1979.

104. G. LIPPMANN, Relations entre les phénomènes électriques et capillaires, *Annales de chimie et de physique*, Vol.5, pp. 494-549, 1875.

105. L.G. LOYTSIANSKIY, *Mekhanika zhidkosti i gaza* (*Mechanics of Fluids and Gases*), in Russian, Gosudarst. Izd. Fiz.-Mat. Literatury, pp. 482-6, Moskva 1959.

106. A. MALAYEV and D.J. NELSON, Extracellular pH modulates the Ca2+ current activated by depletion of intracellular Ca2+ stores in human macrophages, *J. Membr. Biol.*, Vol.146, pp. 101-11, 1995.

107. J.M. MANSOUR and V.C. MOW, The permeability of articular cartilage under compressive strain and at high pressures, *J. Bone Joint Surg.* - American Volume, Vol.58(4), pp. 509-16, 1976.

108. A. A. MARINO and R. O. BECKER, Biological effects of extremely low frequency electrical and magnetic fields: a review, *Physiological Chemistry and Physics*, Vol.9, pp. 131-47, 1977.

109. A.A. MARINO, J.A. SPADORA, E. FUKADA, L.D. KAHN and R.O. BECKER, Piezoelectricity in Collagen Films, *Calcif. Tissue Int.*, Vol.31, pp.257-259, 1980.

110. A. MAROUDAS, H. MUIR and J. WINGHAM, The correlations of fixed negative charge with glycosaminoglycan content of human articular cartilage, *Biochimica et Biophysica*, Vol. 177, pp. 492-500, 1969.

111. A. MAROUDAS, Physicochemical properties of articular cartilage, in: *Adult Articular Cartilage*, ed. by M.A.R. Freeman, Pitman Medical, Kent, UK, 1979.

112. A. MAROUDAS, J. MIZRAHI, E. BENAIM, R. SCHNEIDERMAN, G. GRUSHKO, Swelling pressure of cartilage: role played by proteoglycans and collagen, in: *Mechanics of Swelling: From Clays to Living Cells and Tissues*, NATO ASI Series H: Cell Biology Vol. 64, edited by T.K. Karalis, Springer-Verlag, Berlin and Heidelberg 1992, pp. 487-512.

113. A. MAROUDAS, J. MIZRAHI and E. BENAIM, A study of compressive properties of cartilage using unconfined compression: example of an experimental and theoretical approach, in: *Interstitium, Connective Tissue and Lymphatics*, Proceedings of the XXXII Congress of the International Union of Physiological Sciences, editors R.K. Reed, N.G. McHale, J.L. Bert, C.P. Winlove, G.A. Laine, Portland Press, London 1995, pp.55-65.

114. H. MARSCHNER, *Mineral Nutrition of Higher Plants*, Ed 2. Academic Press, London, 1995.

115. D. J. MASON, R. A. HILLAM and T. M. SKERRY Constitutive in vivo mRNA expression by osteocytes of beta-actin, osteocalcin, connexin-43, IGF-I, c-fos and c-jun, but not TNF-alpha nor tartrate-resistant acid phosphatase, *J. Bone Miner. Res.*, Vol.11, pp. 350-57, 1996.

116. P. MAZUR and J.TH.G. OVERBEEK, On electro-osmosis and streaming potentials in diaphragms, *Rec. Trav. Chim.*, Vol.70, pp. 83-91, 1951.

117. S. MCLAUGHLIN, The electrostatic properties of membranes, *Annu. Rev. Biophys. Biophys. Chem.*, Vol.18, pp. 113-36, 1989.

118. J. VAN MEERVELD and J.M. HUYGHE, Analytical transient solutions of saturated charged porous media, *Bioengineering Conference*, ASME, BED-Vol. Vol.50, pp. 743-44, 2001.

119. J. VAN MEERVELD, M.M. MOLENEAAR, J.M.R.J. HUYGHE and F.P.T. BAAIJENS, Analytical solutions of compression, free swelling and electrical loading of saturated charged porous media, *Transp. Porous Media*, Vol.50, pp.111-26, 2003.

120. A. MIYAUCHI, K.A. HRUSKA, E.M. GREENFIELD, R. DUNCAN, J. ALVAREZ, R. BARATTOLO, S. COLUCCI, A. ZAMBONIN-ZALLONE, S.L. TEITELBAUM, A. TET, Osteoclast cytosolic calcium, regulated by voltage-gated calcium channels and extracellular calcium, controls podosome assembly and bone resorption, *J. Cell Biol.*, Vol.111(6 Pt 1), pp. 2543-52, 1990.

121. A. MIYAUCHI, K. NOTOYA, Y. MIKUNI-TAKAGAKI, Y. TAKAGI, M. GOTO, Y. MIKI, T. TAKANO-YAMAMOTO, K. JINNAI, K. TAKAHASHI, M. KUMEGAWA, K. CHIHARA and T. FUJITA, Parathyroid hormone-activated volume-sensitive calcium influx pathways in mechanically loaded osteocytes, *J. Biol. Chem.*, Vol.275(5), pp. 3335-42, 2000.

122. J. MIZRAHI, A. MAROUDAS, Y. LANIR, I. ZIV and T.J. WEBBER The "instantaneous" deformation of cartilage: effects of collagen fiber orientation and osmotic stress, *Biorheology*, Vol.23(4), pp. 311-30, 1986.

123. M.M. MOLENAAR, J.M. HUYGHE and F.P.T. BAAIJENS, An electro-chemo-mechanical formulation of bone, *Bioengineering Conference ASME, BED*-Vol.50, pp. 423-24, 2001.

124. F.M.M. MOREL and J.G. HERING, *Principles and Applications of Aquatic Chemistry*, John Wiley & Sons, New York, 1993.

125. M.L. MOSS, Bone as a connected cellular network: testing and modeling, *Topics in Biomedical Engineering*, Pergamon Press, 1991.

126. V.C. MOW, M.H. HOLMES, W.M. LAI, Fluid transport and mechanical properties of articular cartilage: a review, *Journal of Biomechanics*, Vol. 17(5), pp.377-94, 1984.

127. V.C. MOW, and A. RATCLIFFE, Structure and functions of articular cartilage and meniscus, in: *Basic Orthopaedic Biomechanics*, ed. by V.C. Mow and W.C. Hayes, pp.275-315, Lippincott-Raven Publishers, Philadelphia, 1997.

128. D. W. MURRAY, N. RUSHTON, The effect of strain on bone cell prostaglandin E2 release: a new experimental method, *Calcif. Tissue Int.*, Vol.47, pp.35-39, 1990.

129. C. NEIDLINGER-WILKE, I. STALL, L. CLAES, R. BRAND, I. HOELLEN, S. RUBENACKER, M. ARAND and L. KINZL, Human osteoblasts from younger normal and osteoporotic donors show differences in proliferation and TGF-β release in response to cyclic strain, *J. Biomech.*, Vol.28, pp.1411-18, 1995.

130. L.J. NG, A. PLAAS, A. GRODZINSKY and C. ORTIZ, Atomic force microscopy studies of the conformation of cartilage aggrecan and related constituents, *Abstracts of Papers ACM*, 224, 131-COLL Part 1, Aug 18, 2002.

131. P.J. NIJWEIDE, R. J. P. MULDER, Identification of osteocytes in osteoblast-like cultures using a monoclonal antibody specifically directed against osteocytes, *Histochemistry*, Vol. 84, pp.343-50, 1986.

132. P.J. NIJWEIDE, E.H. BURGER and J.H. FEYEN , Cells of bone: proliferation, differentiation, and hormonal regulation, *Physiological Reviews*, Vol. 66(4), pp.855-86, 1986.

133. P.J. NIJWEDE and E.H. BURGER, Mechanism of bone formation in vitro, *Bone*, Vol. 1: *The osteoblast and osteocyte*, ed. B.K. Hall, pp. 303-326, The Telford Press, Caldwell, N.J., 1990.

134. P. NOBEL, *Physicochemical and environmental plant physiology*, Academic Press, San Diego CA, 1991.

135. I. OBI, Y. ICHIKAWA, T. KAKUTANI and M. SENDA, Electrophoretic studies on plant protoplasts. I. pH dependence of zeta potentials of protoplasts from various sources, *Plant Cell Physiol.*, Vol.30, pp.439-44, 1989.

136. I. OBI, Y. ICHIKAWA, T. KAKUTANI and M. SENDA, Electrophoresis, zeta potential and surface charges of barley mesophyll protoplasts, *Plant Cell Physiol.*, Vol.30, pp.129-35, 1989.

137. R.W. O'BRIEN and L.R. WHITE, Electrophoretic mobility of spherical colloidal particle, *J. Chem. Soc. Faraday Trans.*, Vol.74, pp.1607-26, 1978.

138. L. ONSAGER, Report on a revision of the conductivity theory, *Trans. Faraday Soc.*, Vol. 23, pp. 341-49, 1927.

139. J.TH.G. OVERBEEK, Electrochemistry of the double layer, in: *Colloid Science*, Vol. I. Irreversible systems, ed. H.R. Kruyt, pp. 115-193, Elsevier, Amsterdam-Houston, 1952.

140. M. OTTER, S. GOHEEN and W.S. WILLIAMS, Streaming potentials in chemically modified bone, *J. Orthop. Research*, Vol. 6, pp. 346-59, 1988.

141. R.G. PACKARD, Streaming potentials across glass capillaries for sinusoidal pressure, *J. Chem. Physics*, Vol. 21(2), pp.303-307, 1953.

142. N. PARKINSON, S. BOLSOVER, W. MASON, Nuclear and cytosolic calcium changes in osteoclasts stimulated with ATP and integrin-binding peptide, *Cell Calcium*, Vol.24(3), pp.213-21, 1998.

143. K. PIEKARSKI, M. MUNRO, Transport mechanism operating between blood supply and osteocytes in long bones, *Nature*, Vol. 269(5623), pp. 80-82, 1977.

144. D. PIENKOWSKI and S.R. POLLACK, The origin of stress-generated potentials in fluid saturated bone, *J. Orthop. Res.*, Vol. 1, pp. 30-41, 1983.

145. S. PRIDE, Governing equations for the coupled electromagnetics and acoustic of porous media, *Phys. Rev.*, Vol. 50(21), pp. 15678-696, 1994.

146. S.R. PRIDE, M.W. HAARTSEN, Electroseismic wave properties, *Journal of the Acoustical Society of America*, Vol. 100(3), pp. 1301-1315, 1996.

147. S.R. PRIDE, S.GARAMBOIS, The role of Biot slow waves in electroseismic wave phenomena, *Journal of the Acoustical Society of America*, Vol. 111(2), pp. 697-706, 2002.

148. S. PRITCHARD, G.R. ERICKSON, and F. GUILAK, Hyperosmotically induced volume change and calcium signaling in intervertebral disk cells: the role of the actin cytoskeleton, *Biophys. J.*, Vol. 83(5), pp. 2502-10, 2002,

149. G. QUINCKE, Ueber die Fortführung materieller Theilchen durch strömende Electricität, *Annalen der Physik und Chemie* (hgb. J.C. Poggendorff), Vol.113, pp.513-598, 1861.

150. G.N. RAMACHANDRAN, Stereochemistry of collagen, *Int. J. Peptide & Protein Res.*, Vol.31(1), pp.1-16, 1988.

151. K.M. REICH, C.V. GAY and J.A. FRANGOS, Fluid shear stress as a mediator of osteoblast cyclic adenosine monophosphate production, *J. Cell. Physiol.*, Vol.143, pp.100-104, 1990.

152. K.M. REICH and J.A. FRANGOS, Protein kinase C mediates flow-induced prostaglandin E−2 production in osteoblasts, *Calcif. Tissue Int.*, Vol.52, pp.62-66, 1993.

153. J.P. REILLY, *Applied Bioelectricity: From Electrical Simulation to Electropathology*, Springer, New York, 1998.

154. P.M. REPPERT, F.D. MORGAN, D.P. LESMES and L. JOUNIAUX, Frequency-dependent streaming potentials, *Journal of Colloid and Interface Science*, Vol.234(1), pp.194-203, 2001.

155. F.F. REUSS, Notice sur un nouvel effet de l'éléctricité galvanique, *Mémoirs de la Societé impériale des naturalistes de Moscou*, Vol.2, pp.327-37, 1808.

156. TH.M. RIDDICK, *Control of Colloid Stability through Zeta Potential*, Library of Congress Catalogue Number 67Ũ18001, Zeta-Meter Inc., 1968.

157. A.G. ROBLING and C.H. TURNER, Mechanotransduction in bone: genetic effects on mechanosensitivity in mice, *Bone*, Vol.31(5), 562-9, 2002.

158. G.D. ROBSON, E. PREBBLE, A. RICKERS, S. HOSKING, D.W. DENNING, A.P. TRINCI and W. ROBERTSON, Polarized growth of fungal hyphae is defined by an alkaline pH gradient, *Fungal Gen. Biol.*, Vol. 20, pp. 289-98, 1996.

159. J.R. ROGERS, Why do bacteria colonize aquifer surfaces? Geochemical and nutrient controls of bacterial colonization of silicate surfaces, http://water.usgs.gov/ogw/pubs/ofr0289/jrr.

160. W. ROOS, S. EVERS, M. HIEKE, M. TSCHÖPE and B. SCHUMANN, Shifts of intracellular pH distribution as a part of signal mechanism leading to the elicitation of benzophenanthridine alkaloids - Phytoalexin biosynthesis in cultured cells of Eschscholtzia californica, *Plant Physiol.*, Vol.118, pp.349-64, 1998.

161. C.T. RUBIN, K.J. MCLEOD and S.D. BAIN, Functional strains and cortical bone adaptation: epigenetic assurance of skeletal integrity, *J. Biomech.*, Vol. 23, suppl. 1, pp. 43-54, 1990.

162. C.T. RUBIN and K.J. MCLEOD, Inhibition of osteopenia by biophysical intervention, in: *Osteoporosis*, Eds: R. Marcus, J. Kelsey & D. Feldman., pp. 351-71, Academic Press, New York, 1996.

163. J. RUBIN, K.J. MCLEOD, L. TITUS, M.S. NANES, B.D. CATHERWOOD and C.T. RUBIN, Formation of osteoclast-like cells is suppressed by low frequency, low intensity electric fields, *J. Orthop. Res.*, Vol. 14(1), pp. 7-15, 1996.

164. C. RUBIN, A.S. TURNER, S. BAIN, C. MALLINCKRODT and K. MCLEOD, Anabolism. Low mechanical signals strengthen long bones, *Nature*, Vol.412(6847), 603-4, 2001.

165. D.M. SALTER, J.E. ROBB and M.O. WRIGHT, Electrophysiological responses of human bone cells to mechanical stimulation: evidence for specific integrin function in mechanotransduction. *J. Bone Miner. Res.*, Vol.12(7), 1133-41, 1997.

166. R.A. SALZSTEIN, S.R. POLLACK, A.F.T. MAK and N. PETROV, Electromechanical potentials in cortical bone – I. A continuum approach, *J. Biomech.*, Vol.20, pp.261-70, 1987.

167. R.A. SALZSTEIN and S.R. POLLACK, Electromechanical potential in cortical bone – II. Experimental analysis, *J. Biomech.*, Vol.20, pp.271-80, 1987.

168. A. C. SCOTT and N. STRÖMGREN ALLEN, Changes in cytosolic pH within Arabidopsis root columella cells play a key role in the early signaling pathway for root gravitropism, *Plant Physiol.*, Vol.121(4), pp.1291Ũ98, 1999.

169. R. SCHNEIDERMAN, D. KERET and A. MAROUDAS, Effects of mechanical and osmotic pressure on the rate of glycosaminoglycan synthesis in the human adult femoral head cartilage: an in vitro study, *Journal of Orthopaedic Research*, Vol.4(4), pp.393-408, 1986.

170. R.L. SMITH, B.S. DONLON, M.K. GUPTA, M. MOHTAI, P. DAS, D.R. CARTER, J. COOKE, G. GIBBONS, N. HUTCHINSON, D.J. SCHURMAN, Effects of fluid-induced shear on articular chondrocyte morphology and metabolism in vitro, *Journal of Orthopaedic Research*, Vol. 13(6), pp.824-31, 1995.

171. M. SMOLUCHOWSKI, Contribution à la théorie de l'endosmose electrique et de quelques phénomènes corrélatifs, *Bull. Acad. Sci. Cracovie*, Cl. Sci. Math. et Natur., Vol.63, pp.110-127 (in Polish), 182-199 (in French) (1903); also *Pisma Marjana Smoluchowskiego - Oeuvres de Marie Smoluchowski*, wyd. Wł. Natanson i J. Stock, Acad. Pol. Sci. Lett., Cracovie, Librairie Polytechnique, Ch. Béranger, Paris, t.I, pp.384-420, 1924.

172. M. SMOLUCHOWSKI, Elektrische Endosmoze und Strömungsströme, in: *Handbuch der Elektrizität und des Magnetismus*, ed. by J. A. Barth, vol. II, pp. 366-428, Leipzig 1914; also: *Pisma*, t. III, pp. 246-346, 1928.

173. R. SMOLUCHOWSKI, Work function and double layer, *Phys. Rev.*, Vol.59, pp.944, 1941.

174. M.A. SOLTZ and G.A. ATESHIAN, A conewise linear elasticity mixture model for the analysis of tension-compression nonlinearity in articular cartilage, JOURNAL OF BIOMECHANICAL ENGINEERING, Vol.122(6), pp.576-86, 2000.

175. J. SOULHAT, M.D. BUSCHMANN, A. SHIRAZI-ADL, A fibril-network-reinforced biphasic model of cartilage in unconfined compression, JOURNAL OF BIOMECHANICAL ENGINEERING, Vol.121(3), pp.340-7, 1999.

176. A.A. SPIRT and S.R. POLLACK, Age-related change in the zeta potential of bone and its influence upon endogenous electrical field strength, in: *Electricity and magnetism in biology and medicine*, edited by M. Blank, pp.693-97, San Francisco Press, San Francisco, 1993.

177. J.M. SQUIRE, M. CHEW, G. NNEJI, C. NEAL, J. BARRY and C. MICHEL, Quasi-periodic substructure in the microvessel endothelial glycocalyx: a possible explanation for molecular filtering?, *J. Structural Biology*, Vol.136(3), pp.239-55, 2001.

178. W. STARKEBAUM, S.R. POLLACK and E. KOROSTOFF, Microelectrode studies of stress generated potentials in four point bending of bone, *J. Biomed. Mat. Res.*, Vol.13(5), pp.729-51, 1979.

179. R. STECK, P. NIEDERER, M.L. KNOTHE TATE, A finite element analysis for the prediction of load-induced fluid flow and mechanochemical transduction in bone, *J. Theor. Biol.*, Vol.220(2), pp.249-59, 2003.

180. J.V. STEIDL and A.J. YOOL, Differential sensitivity of voltage-gated potassium channels Kv1.5 and Kv1.2 to acidic pH and molecular identification of pH sensor, *Mol. Pharmacol.*, Vol.55, pp.812-20, 1999.

181. O. STERN, Zur Theorie der elektrolytischen Doppelschicht, *Z. Elektrochem.*, Vol.30, pp.508-16, 1924.

182. C.G. SUMMER and D.C. HENRY, Cataphoresis. Part II.- A new experimental method, and a confirmation of Smoluchowski's equation, *Proc. R. Soc. London*, Vol.133A, pp.130-40, 1931.

183. K. SUPRENANT, Unidirectional microtubule assembly in cell-free extracts of Spisula solidissima oocytes is regulated by subtle changes in pH, *Cell Motility and the Cytoskeleton*, Vol.19, pp.207-20, 1991.

184. C.C. SWAN, R.S. LAKES, R.A. BRAND and K.J. STEWART, Micromechanically based poroelastic modeling of fluid flow in Haversian bone, *J. Biomech. Eng.*, Vol.125(1), pp.25-37, 2003.

185. P. SZYMANSKI, Quelques solutions exactes des équations de l'hydrodynamique du fluide visqueux dans le cas d'un tube cylindrique, *Journal de Mathématiques pures et appliquées*, Vol.11(9), pp.67-107, 1932.

186. J. TAFEL, Über die Polarisation bei kathodischer Wasserstoffentwicklung, *Zeitschrift Phys. Chem.*, Vol.50, pp.641-712, 1905.

187. K. TANAKA, T. MATSUO, M. OHTA, T. SATO, K. TEZUKA, P. J. NIJWEIDE, Y. KATOH, Y. HAKEDA and M. KUMEGAWA Time-lapse microcinematography of osteocytes, *Miner. Electrolyte Metab.* Vol.21, pp.189-92, 1995.

188. J.J. TELEGA and R. WOJNAR, Flow of conductive fluids through poroelastic media with piezoelectric properties, *Fluid-structure interactions in biomechanics* EUROMECH344, 10-13th April 1996, Imperial College, London, 1996.

189. J.J. TELEGA and R. WOJNAR, Flow of conductive fluids through poroelastic media with piezoelectric properties, *J. Theor. Appl. Mech.*, Vol.36, pp.775-94, 1998.

190. J.J. TELEGA and R. WOJNAR, Piezoelectric effects in biological tissues, *J. Theor. Appl. Mech.*, Vol.40, pp.723-59, 2002.

191. R.-Y. TSAY and S. WEINBAUM, Viscous flow in a channel with periodic cross-bridging fibers: exact solution and Brinkman approximation, *J. Fluid Mech.*, Vol.226, pp.125-48, 1991.

192. C.H. TURNER, M.R. FORWOOD and M.W. OTTER, Mechanotransduction in bone: do bone cells act as sensors of fluid flow?, *The FASEB Journal*, Vol.8, pp.875-78, 1994.

193. C.H. TURNER, T. YOSHIKAWA, M.R. FORWOOD, T.C. SUN and D.B. BURR, High frequency components of bone strain in dogs measured during various activities. *J. Biomech.* Vol.28(1), pp.39-44, 1995.

194. C.H. TURNER, Y. TAKANO, I. OWAN and G.A. MURRELL, Nitric oxide inhibitor L-NAME suppresses mechanically induced bone formation in rats, *American J. Physiol.*, Vol.270(4) Pt 1, pp.E634-9, 1996.

195. A. VAN DER PLAS and P. J. NIJWEIDE, Isolation and purification of osteocytes, *J. Bone Miner. Res.*, Vol.7, pp.389-96, 1992.

196. D. VELEGOL, J.D. FEICK and L.R. COLLINS, Electrophoresis of spherical particles with a random distribution of zeta potential or surface charge, *Journal of Colloid and Interface Science*, Vol.230, pp.114-21, 2000.

197. D. VELEGOL, Electrophoresis of randomly charged particles, *Electrophoresis*, Vol.23(13), pp.2023-8, 2002.

198. E.J. VERWEY and J.TH.G. OVERBEEK, *Theory of the Stability of Lyophobic Colloids*, Elsevier, Amsterdam 1948.

199. S. WEINBAUM, S.C. COWIN and YU ZENG, A model for the excitation of osteocytes by mechanical loading-induced bone fluid shear stresses, *J. Biomech.*, Vol.27, pp.339-60, 1994.

200. S. WEINBAUM, P. GUO and L. YOU, A new view of mechanotransduction and strain amplification in cells with microvilli and cell processes, *Biorheology*, Vol.38(2-3), pp.119-42, 2001.

201. S. WEINBAUM, X. ZHANG, Y. HAN, H. VINK, S.C. COWIN, Mechanotransduction and flow across the endothelial glycocalyx, *Proc. of the National Ac. of Sci. of the USA*, Vol.100(13), pp.7988-95, 2003.

202. G. WIEDEMANN, Ueber die Bewegung von Flüssigkeiten im Kreise der geschlossen galvanischen Säule, *Ann. Phys. Chemie* (J.C. Poggendorff), Vol.87, pp.321-52, 1852.

203. R. WOJNAR and J.J. TELEGA, Electrokinetics in dielectric porous media, in: *Problems of Environmental and Damage Mechanics*, edit. W. Kosiński, R. de Boer, D. Gross, pp.97-136, Wydawnictwa IPPT PAN, Warszawa, 1997.

204. C.E. YELLOWLEY, C.R. JACOBS, Z. LI, Z. ZHOU, H.J. DONAHUE , Effects of fluid flow on intracellular calcium in bovine articular chondrocytes, *American Journal of Physiology*, Vol. 273(1 Pt 1), pp.C30-6, 1997.

205. C.E. YELLOWLEY, J.C. HANCOX, H.J. DONAHUE, Effects of cell swelling on intracellular calcium and membrane currents in bovine articular chondrocytes, *Journal of Cellular Biochemistry*, Vol. 86(2), pp.290-301, 2002.

206. U. YERMIYAHU, SH. NIR, G. BEN-HAYYIM, U. KAFKAFI and TH.B. KINRAIDE, Root elongation in saline solution related to calcium binding to root cell plasma membranes, *Plant and Soil*, Vol.191(1), pp.67-76, 1997.

207. N. YONEZAWA, E. NISHIDA and H. SAKAI, pH control of actin polymerization by cofilin, *J. Biol. Chem.*, Vol.260, pp.14410-12, 1985.

208. L.D. YOU, S. WEINBAUM, S.C. COWIN and M.B. SCHAFFLER, A new understanding of osteocyte process ultrastructure, *Conference Proceedings of Second Joint EMBS-BMES Conference 2002*, 24th Annual Intern. Confer. of the Engineering in

Medicine and Biology Society, Annual Fall Meeting of the Biomedical Engineering Society, IEEE, vol.1, pp. 589-90, Piscataway NJ 2002.

209. YOUNG-JO KIM, L.J. BONASSAR and A.J. GRODZINSKY, The role of cartilage streaming potential, fluid flow and pressure in the stimulation of chondrocyte biosynthesis during dynamic compression, *J. Biomech.*, Vol.28(9), pp.1055-66, 1995.

210. D.L. YPEY, A.F. WEIDEMA, K.M. HOLD, A. VAN DER LAARSE, J.H. RAVESLOOT, A. VAN DER PLAS and P.J. NIJWEIDE, Voltage, calcium, and stretch activated ionic channels and intracellular calcium in bone cells, *J. Bone & Mineral Res.*, Vol.7(Dec.), Suppl 2, pp.S377-87, 1992.

211. Y. ZENG, S.C. COWIN and S. WEINBAUM, A fiber matrix model for fluid flow and streaming potentials in the canaliculi of an osteon, *Annals of Biomed. Eng.*, Vol.22(3), pp.280-92, 1994.

212. D. ZHANG, S.C. COWIN and S. WEINBAUM, Electrical signal transmission and gap junction regulation in a bone cell network: a cable model for an osteon, *Annals of Biomed. Eng.*, Vol.25(2), pp.357-74, 1997.

213. S. ZIMMERMANN, T. EHRHARDT, G. PLESCH, B. MULLER-ROBER, Ion channels in plant signaling, *Cell Mol. Life Sci.*, Vol.55, pp.183-203, 1999.